Earth-Science Reviews 156 (2016) 14–38

Contents lists available at ScienceDirect

Earth-Science Reviews

journal homepage: www.elsevier.com/locate/earscirev

Temporal behavior of deep-seated gravitational slope deformations: A review

Tomáš Pánek [a,*], Jan Klimeš [b]

[a] Department of Physical Geography and Geoecology, Faculty of Science, University of Ostrava, Chittussiho 10, 710 00 Ostrava, Czech Republic
[b] Institute of Rock Structure and Mechanics, Academy of Sciences of the Czech Republic, V Holešovičkách 41, Prague 8 182 09, Czech Republic

ARTICLE INFO

Article history:
Received 13 May 2015
Received in revised form 2 February 2016
Accepted 22 February 2016
Available online 2 March 2016

Keywords:
Deep-seated gravitational slope deformations
Catastrophic slope failures
Deformation rates
Dating
Monitoring

ABSTRACT

Deep-seated gravitational slope deformations (DSGSDs) are slow moving, hillslope-scale mass movements featuring characteristic landforms such as double-crested ridges and upslope-facing scarps that occur in diverse landscapes throughout the world. Although these deformations have been studied since the 1960s, significant insights to the rates of DSGSDs have only been gained within the last two decades owing to progress in geochronology, remote sensing and instrumental monitoring. Absolute age and monitoring data indicate that DSGSD movements are observable over long-term ($\geq 10^2$ years) and short-term ($<10^2$ years) intervals. Apart from creep, an episodic deformation also plays a crucial role, especially in regions with earthquakes and heavy rainfall. Our review also supports the notion of DSGSDs as precursors of catastrophic rock slope failures, given that many of the world's largest rock avalanches have occurred in areas with diagnostic DSGSD features, indicating that sudden collapse was preceded by a prolonged stage of slope sagging. Detailed studies on DSGSDs have therefore the potential for better prediction of catastrophic rock slides and rock avalanches.

Future research directions include constraining the lifespan of DSGSDs with absolute age dating and precise high-resolution monitoring of spatio-temporal displacement across DSGSD bodies. It is of great importance to include absolute time scales in the numerical models of DSGSDs. Furthermore, combining remote sensing techniques such as Synthetic Aperture Radar Interferometry with high-resolution LiDAR scanning and near-surface geophysics offers a promising toolkit for collecting very detailed and accurate data on the short-term deformation rates of DSGSDs.

Contents

* Corresponding author.
E-mail address: tomas.panek@osu.cz (T. Pánek).

http://dx.doi.org/10.1016/j.earscirev.2016.02.007
0012-8252/

1. Introduction

Deep-seated gravitational slope deformations (DSGSDs; Agliardi et al., 2001) are generic terms for slow moving rock-mass movements that encompass entire hillslopes or valley flanks (Dramis and Sorriso-Valvo, 1994; Agliardi et al., 2012). Comparable phenomena also occur in some extraterrestrial settings (Mège and Bourgeois, 2011; Guallini et al., 2012). DSGSDs create characteristic landform assemblages such as double-crested ridges, trenches, synthetic and antithetic (uphill-facing) scarps, tension cracks and convex (bulged) toes. Apart from their substantial geomorphic imprint (Korup, 2006; Agliardi et al., 2013) and contributions to the diversity of mountain landscapes (Alexandrowicz and Margielewski, 2010), DSGSDs are also significant natural hazards (Dramis and Sorriso-Valvo, 1994). Even very slowly moving DSGSDs may damage local infrastructure (Ambrosi and Crosta, 2006), although it is the acceleration of slope movements to potential catastrophic failures that may endanger mountain communities (Chigira et al., 2010). The hazards associated with DSGSDs are of concern to geoscientists, civil engineers, social scientists and civil protection specialists.

In the last decade, the number of studies on DSGSDs has grown substantially. Numerous case studies from places such as Alaska, the Pacific Coast Mountains, the Rocky Mountains, the Andes, the European Alps, the Pyrenees, the Apennines, the Carpathians, the Ethiopian Highland, the Himalaya, the Japanese Alps, and New Zealand (Fig. 1) reveal that DSGSDs are far from rare, yet they are rather characteristic features of mountain belts. Reports on DSGSDs come from a full spectrum of terrain, ranging from low-relief isolated mountains (e.g., Mège et al., 2013) to Earth's highest mountain ranges (e.g., Shroder et al., 2011). Recent progress in geophysical techniques and physical and numerical modeling (e.g., Bachmann et al., 2009; Barla et al., 2010) has provided valuable insights into the internal structure and mechanics of DSGSDs. The first mountain belt-scale inventories of DSGSDs (Agliardi et al., 2012, 2013; Crosta et al., 2013) provide information regarding the details of spatial distribution, including the relationships with geologic structures, neotectonics, geomorphometry, deglaciation patterns, and long-term ($>10^6$ years) landscape evolution. Amidst all this progress, temporal dynamics remains one of the least explored aspects of DSGSDs. Although methods such as geochronology (e.g. terrestrial cosmogenic nuclide/TCN dating) and monitoring techniques (e.g. Global Navigation Satellite System and Synthetic Aperture Radar Interferometry) have become routine since the 1990s providing new insights into the temporal evolution of DSGSDs (e.g., Ambrosi and Crosta, 2006; Hippolyte et al., 2012; Strozzi et al., 2013), general understanding of their temporal dynamics remains elusive.

Here we review the state-of-the-art and current key issues regarding the temporal behavior of DSGSDs. This study is motivated by a growing number of studies that address long- and short-term DSGSD dynamics (Fig. 1) and by the introduction of new techniques that allow for a much wider insight into the chronology and recent activity of DSGSDs. We relate our review to three guiding questions:

(i) How has recent progress in dating and monitoring techniques stimulated the knowledge of the temporal dynamics of DSGSDs?
(ii) How do DSGSDs evolve over long-term ($\geq 10^2$ years) and short-term ($<10^2$ years) intervals?
(iii) Are DSGSDs prone to catastrophic collapse or able to condition slope susceptibility to catastrophic collapse?

To address these questions, we combine our own experience in DSGSD research (e.g., Pánek et al., 2009a; 2011a, b; 2013; Klimeš et al., 2012) with an extensive review of papers on DSGSDs published since the 1990s when data regarding the temporal behavior of DSGSDs first started to emerge.

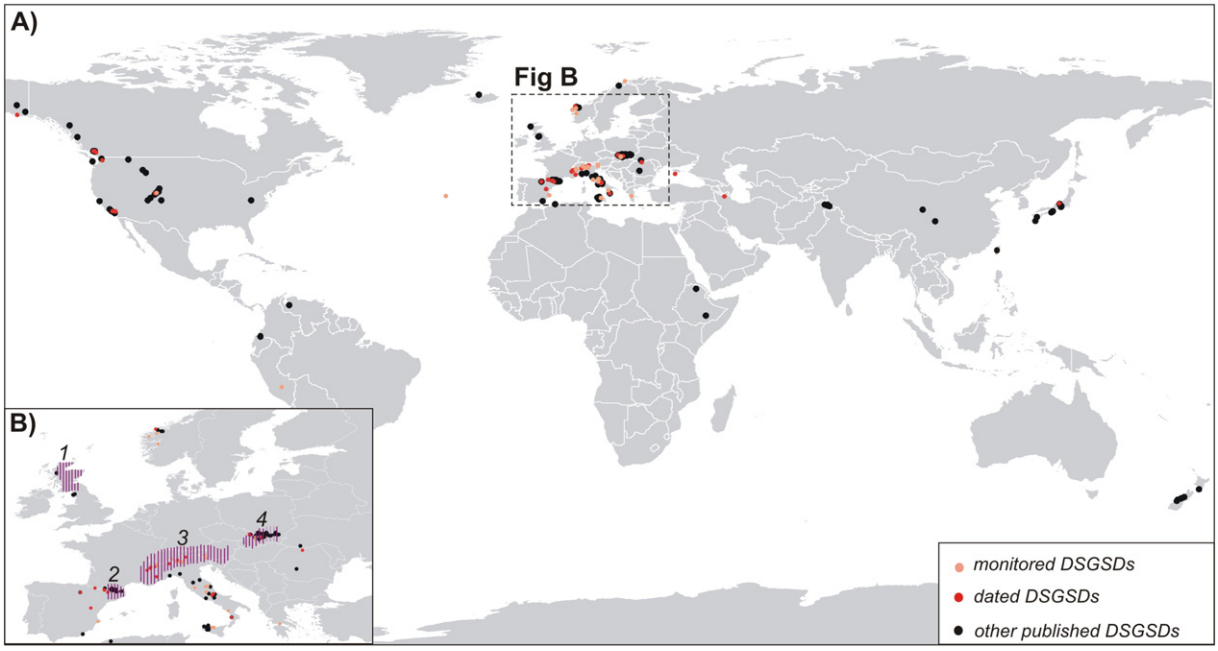

Fig. 1. Distribution of the significant DSGSDs, especially cases from studies published since 1990s. A. Worldwide context. B. Detailed view of Europe. The numbered hatched regions contain widespread databases of DSGSDs published in one or few summarized studies: 1. Scottish Highland (n = 89; Jarman, 2006); 2. Eastern Pyrennes (n = 30; Jarman et al., 2014); 3. European Alps (n = 1033; Crosta et al., 2014); Western Carpathians (>100 cases; Němčok, 1982; Alexandrowicz and Alexandrowicz, 1988).

2. Terminology and formation of DSGSDs

The term 'deep-seated gravitational slope deformation' was most likely first used by Malgot (1977) to describe large-scale gravitational spreading of brittle, neovolcanic rocks overlying plastic Palaeogene and Neogene rocks in the Western Carpathians of Slovakia. The acronym 'DSGSD' was introduced much later, particularly following the studies of Dramis and Sorriso-Valvo (1994) and Agliardi et al. (2001). DSGSDs are not explicitly included as a single category in standard classifications of mass movements (e.g., Cruden and Varnes, 1996, Hungr et al., 2014). Thus, to clarify the subject of this study, we first explain the terminology and provide an overview of the diverse types of mechanisms and settings in which DSGSDs occur.

2.1. Definition of DSGSDs

DSGSD is a non-genetic term referring to specific characteristics of rock-mass movements that affect high-relief mountain slopes that move and deform in extensional, shearing or mixed mode at low rates (mm $year^{-1}$) over long periods. DSGSDs reach considerable thickness (usually of several tens of meters or more) and often lack clearly defined boundaries (Agliardi et al., 2001, 2012; Crosta et al., 2013). Although some researchers also consider the absence of a continuous sliding surface as a diagnostic feature (Dramis and Sorriso-Valvo, 1994), in this review we disregard this criterion and rather follow the approach of Agliardi et al. (2001) who suggest that some alpine DSGSDs contain well developed basal sliding surfaces. In most cases, DSGSDs develop within highly anisotropic rocks and are controlled by inherited structures, such as faults, fold axes, bedding planes, and foliations (Agliardi et al., 2001, 2009b, Pánek et al., 2011a). Characteristic morphostructures of DSGSDs include double ridges, trenches, tension cracks, uphill-facing scarps (i.e. counter scarps or antislope scarps) and downthrown blocks in the upper and middle sectors of slopes and buckling folds, toe bulging, enhanced rock fracturing and secondary mass movements (e.g. landslides and rockfalls) in the middle and lower sectors of slopes (Agliardi et al., 2001) (Fig. 2).

2.2. Mechanisms and types of DSGSDs

From the genetic and kinematic points of view, DSGSDs include a relatively wide variety of slope deformations. Agliardi et al. (2012) offer an extensive review of these mechanisms. However, in this article we focus especially on a sackung (the plural form is sackungen; Zischinsky, 1966, 1969) and large-scale lateral spreading of rock masses which are among the most common deformations forming DSGSDs.

Sackung, i.e. sagging of mountain ridges or rock flow (Cruden and Varnes, 1996 or Dikau et al., 1996), predominantly involves layered metamorphic, igneous and sedimentary rocks in mountain areas (Agliardi et al., 2012). Characteristic structures include systems of gravitational faults that dip steeply into the ridge or sets of predominantly synthetic faults that dip in the same direction as the main slope. Beck (1968); Fig. 2A, B) termed these arrangements symmetric and asymmetric sackung, respectively. Sackungen often result from the paraglacial relaxation of rock massifs following glacial retreat (Agliardi et al., 2001), although they may also occur in areas that have not been glaciated (Fig. 2C). Dynamic loading during earthquakes is a common trigger for initiating (Jibson et al., 2004) or accelerating (Moro et al., 2007) sackungen, which partly explains the abundance of sackungen along active faults (Fig. 2D). Recent studies show that sackungen may also originate from land subsidence following karstification in limestone areas (Pánek et al., 2009b; Apuani and Corazzato, 2009; Lenti et al., 2012; Fig. 2E) or dissolution of evaporites at depth (Gutiérrez et al., 2012a; Carbonel et al., 2013).

In addition to originating from sackungen, DSGSDs may also form from large-scale lateral spreading (Fig. 2F) in mechanically strong sedimentary or volcanic rocks that overlie ductile rocks; such as limestone overlying clay or clayey shale (Dikau et al., 1996). Due to the unconfined ductile lateral flow of the underlying soft rocks, the more rigid cap rocks accommodate strain by developing tension cracks, trenches and scarps, which often evolve into surficial topples, rockfalls or landslides. Consequently, these landforms are sometimes difficult to distinguish from similar features produced by sackungen. Lateral spreading also affects relatively thin slabs of brittle rock that overlie plastic rock in subdued low-relief terrain (e.g., Mantovani et al., 2013), but we limit our review to large-scale cases that are located in mountainous terrain and extend to at least several tens of meters in depth (e.g., Rohn et al., 2004; Gutiérrez et al., 2012 a, b; Fig. 2F).

Besides sackung and lateral spreads, other mechanisms commonly associated with the formation of DSGSDs include flexural and block toppling (Bovis, 1982; Reitner and Linner, 2009) and less often incipient planar sliding (Bovis and Evans, 1996; Pánek et al., 2011a).

The term DSGSD cannot belie its transitional character. Moreover, distinction from large slow-moving landslides that affect substantial parts of mountain slopes and have similar landforms remains difficult (Crosta et al., 2013). For this reason, we include some examples of DSLs in our review and distinguish between the temporal behavior of DSGSDs and that of DSLs. In contrast to DSGSDs, deep-seated landslides (DSLs) have rather distinct boundaries with pronounced head scarps, smaller width/length ratio, limited length with respect to slope dimension and greater internal deformation and fragmentation (Agliardi et al., 2012; Fig. 2G).

DSGSDs and DSLs have recently even been identified in extraterrestrial settings, particularly on Mars (Fig. 2H; Mège and Bourgeois, 2011; Guallini et al., 2012). These Martian examples are at least one order of magnitude larger than their terrestrial equivalents (Kromuszczyńska et al., 2014).

3. Methodological approaches: traditional techniques and recent trends

Recent progress in deciphering the temporal pattern of DSGSDs is closely tied to the development and accessibility of new methods. Among many advances, we highlight (i) the increasing availability and introduction of new dating methods (e.g. Gosse and Phillips, 2001; Dunai, 2010); (ii) the boom in geodetic and remote sensing techniques, mainly in the wider application of Global Positioning System, Global Navigation Satellite System and Interferometric Synthetic Aperture Radar (e.g. Colesanti and Wasowski, 2006); and (iii) improvements in the field of instrumental monitoring (Barla et al., 2010; Klimeš et al., 2012). Significant steps have been made toward understanding time constraints, longevity, character of movements, and the detection of very slow ($<10^{-1}$ mm $year^{-1}$) displacements which are typical of DSGSDs (Table 1). However, in comparison with landslides or earthquake-induced surface deformations, the application of dating and monitoring techniques is still rather rarely applied to DSGSDs. Methods of investigating DSGSDs address vastly different time scales, and we distinguish here long-term ($\geq 10^2$ years) from short-term ($<10^2$ years) studies.

3.1. Methods for inferring long-term ($\geq 10^2$ years) dynamics of DSGSDs

The evolution of DSGSDs over centuries or millennia is difficult to capture using direct instrumental measurements. Therefore, all available information relies on geochronological and stratigraphical methods (Pánek, 2015), which have seen innovations and improvements in both precision and temporal coverage (Table 1; Walker, 2005). As the application of absolute dating methods for timing of DSGSDs is still in its infancy, we summarize the specific requirements, potentials and limitations of these methods in Table 1.

Among the traditional procedures is trenching, derived from classic palaeoseismologic trenching (McCalpin, 2009), and augmented by mostly ^{14}C or OSL dating of dislocated layers (Fig. 3; McCalpin and

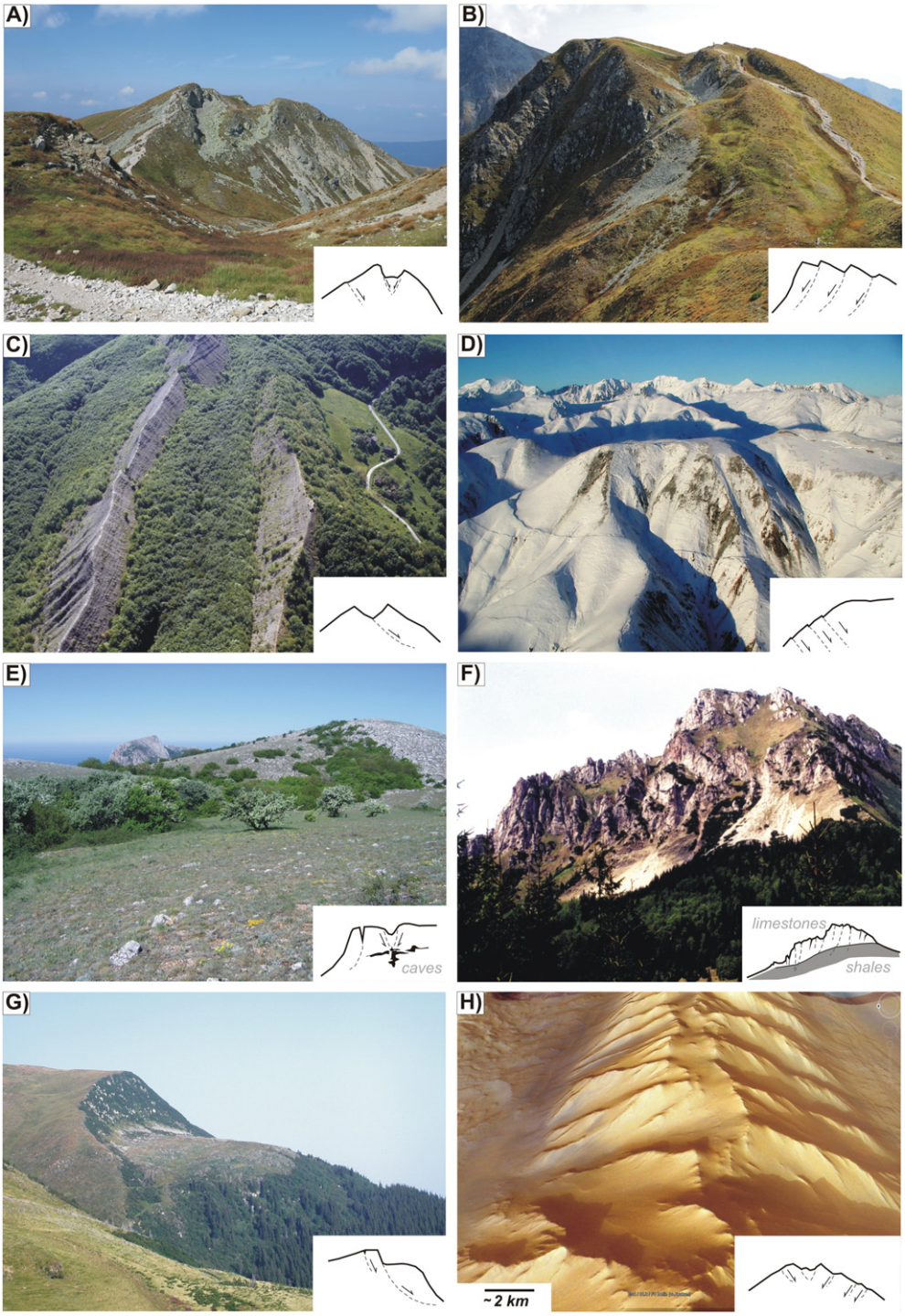

Fig. 2. Examples of frequently occurring modes of DSGSDs from various types of landscapes. A. Ridge-top graben affecting granodiorites of the Salatín Mt. (Tatra Mts., Slovakia). B. Asymmetric sackung (ridge displacement to the left) affecting SE part of the Salatín ridge (Tatra Mts, Slovakia). Cases A and B are examples of DSGSDs situated in mountains that were heavily glaciated during the Late Pleistocene (final deglaciation about 11 ka; Makos et al., 2014) C. Nearly 3 km long double ridge on non-glaciated flysch terrain (Mt. Barigazzo, Northern Apennines, Italy; photo courtesy: G. Bertolini). D. Series of uphill-facing scarps at the Gilette Pass (Alaska, USA) produced by the 2002 Denali Fault earthquake. (Photo courtesy: U.S. Geological Survey/photo by Peter Haeussler). E. Trench in the upper part of DSGSD originated within intensively karstified Jurassic limestones of the Crimean Mountains (Ukraine). F. Mountain-scale lateral spreading of Triassic limestones thrusted over ductile Early Cretaceous marls and shales (non-glaciated terrain of the Rozsutec Mt. — Malá Fatra Mts., Slovakia). G. Short-traveled deep-seated landslide in the SE slope of the Pietrosh Mt. originated within the Mesozoic flysch (Eastern Carpathians, Ukraine). H. Extraterrestrial example of the DSGSD. Google Earth image of the crestal graben at Geryos Montes/Mars.

Irvine, 1995; Thompson et al., 1997; McCalpin and Hart, 2003; Tibaldi et al., 2004; Gutiérrez-Santolalla et al., 2005; Gutiérrez et al., 2008, 2012a, b; Tibaldi and Pasquarè, 2008; Agliardi et al., 2009a; McCalpin et al., 2011; Pánek et al., 2011a; Carbonel et al., 2013). Trenching enables detailed structural–geological, stratigraphical, and geochronological analyses of artificial pits dug across DSGSD lineaments, primarily synthetic scarps, upslope-facing scarps and infilled tension cracks. The most commonly studied features that are used as indicators of former deformation include the geometry and the number of gravitational faults, the orientation of the deformed strata, post-deformation sedimentary infill, and colluvial wedges with dateable material (Fig. 3). In the absence of dateable material, detailed studies of deformation

Table 1
Major dating methods for an estimation of long-term (≥10^2 years) DSGSD dynamics.

Dating method[a]	Requirements	Potentials	Limitations	References of the most important studies
Tephrochronology ($^{40}Ar/^{39}Ar$)	• Tephra layers overlying and/or deformed by DSGSDs	• Potentially provides ages of DSGSDs across the entire Quaternary time range • Possibility to infer DSGSD slip rates	• Applicable only in volcanic areas and their immediate surroundings • Tephra exploitable mostly by trenching or boring — logistic problems in remote mountainous areas	Beget (1985)
TCN (^{10}Be, ^{26}Al, ^{36}Cl, ^{21}Ne, ^{3}He)	• Bedrock surfaces caused by DSGSD movements (downhill- and uphill-facing scarps etc.) without evidence of post-deformation erosion	• Potentially provides ages of DSGSDs across a substantial part of the Quaternary time range • Widespread applicability (easy sampling, common target minerals, frequent occurrence of bedrock scarps) • Dating of vertical sequences on scarps — possibility to infer DSGSD slip rates	• Erosion leads to underestimation of age of scarps • Difficult to evaluate the effect of weathering and erosion on very old exposed scarps (>10^4–10^5 years)	Bigot-Cormier et al. (2005) Hippolyte et al. (2006, 2009, 2012); Le Roux et al. (2009); Sanchez et al. (2010); Hermanns et al. (2013); Zerathe et al. (2013, 2014); Lebourg et al. (2014)
Luminescence (TL, OSL, TT-OSL)	• Fine-grained deposits (containing quartz and feldspar) overlying and/or deformed by DSGSDs	• Potentially provides ages of DSGSDs across the Middle Pleistocene to recent times • Possibility to infer DSGSD slip rates	• Incomplete bleaching of material in a high-energy slope environment • Material for dating exploitable mostly by trenching or boring — logistic problems in remote mountainous areas	Tibaldi and Pasquarè (2008) McCalpin et al. (2011); Gutiérrez et al. (2012b)
U-series ($^{230}Th/^{234}U$, $^{231}Pa/^{235}U$, $^{234}U/^{238}U$)	• Speleothems or other secondary crystallized carbonates infilling cracks or covering DSGSD scarps	• Enable to cover the whole time span of DSGSDs from the opening of initial cracks • Potentially provides ages of DSGSDs across the Middle Pleistocene to recent times	• Applicable only for some types of DSGSDs (esp. lateral spreading) developed in carbonate rocks • Detrital contamination (e.g. by ^{230}Th, ^{234}U, ^{238}U) is common for exposed and weathered speleothems	Pánek et al. (2009b)
Radiocarbon (^{14}C)	• Organic deposits overlying and/or deformed by DSGSDs	• High precision (10^0–10^2 years) of dating across a time range of 10^3–10^4 years • Possibility to infer DSGSD slip rates	• Many DSGSDs are older than the effective time range of radiocarbon dating • Lack of organic material within deposits overlying DSGSDs • Organic material exploitable mostly by trenching or boring — logistic problems in remote mountainous areas	McCalpin and Irvine (1995); Thompson et al. (1997); McCalpin and Hart (2003); Tibaldi et al. (2004); Gutiérrez-Santolalla et al. (2005); Gutiérrez et al. (2008; 2012a,b); Tibaldi and Pasquarè (2008); Agliardi et al. (2009a); Carbonel et al. (2013)
Lichenometry	• Suitable species of lichens (esp. *Rhizocarpon sp.*) growing on exposed bedrock surfaces (DSGSD scarps etc.)	• High precision dating of newly exposed DSGSD surfaces back to 10^1–10^2 years • Covers temporal gaps between effective time ranges of monitoring and radiometric dating	• Applicable for absolute dating only if the lichen growth rate for the particular region is known (general scarcity of calibration surfaces)	Bovis (1982)
Dendrochronology	• Suitable trees (esp. conifers) growing on DSGSD morphostructures (grabens, open cracks, uphill-facing scarps etc.)	• High, seasonal precision of dating DSGSD movements back to 10^0–10^2 years • Covers temporal gaps between effective time ranges of monitoring and radiometric dating	• Alpine DSGSDs are frequently located above the tree-line • Low sensitivity of trees to recording deep-seated movements	Fantucci and Sorriso-Valvo (1999)

[a] Ordered in respect to available time range.

structures and their relationships with younger sediment infill may still reveal valuable information on the relative chronology, the number of deformation events, and the continuous or episodic nature of movements (Agliardi et al., 2009a). Methods such as AMS ^{14}C and OSL allow dating of complex sedimentary assemblages that may contain only very small organic fragments or inorganic colluvial or palustrine layers (McCalpin et al., 2011).

Work on the long-term evolution of DSGSDs is now feasible using TCN dating. The application of cosmogenic ^{10}Be (Hippolyte et al., 2006, 2009, 2012; Le Roux et al., 2009; Sanchez et al., 2010) and ^{36}Cl (Zerathe et al., 2013, 2014) exposure dating has returned very promising results on the timing of DSGSDs and DSLs. The dating of multiple samples of rocks exposed in the vertical profiles of scarps provides constraints on the onset, former dynamics and termination of DSGSD (Hippolyte et al., 2009, 2012; Le Roux et al., 2009). In comparison with trenching, which mainly relies on the presence of a sag ponds or other natural depressions likely to contain sedimentary fills, TCN dating requires the presence of an exposed bedrock scarp, which is common within many DSGSDs bodies. Both trenching and TCN dating help to determine slip rates and the onset of motion in ideal circumstances (McCalpin and Irvine, 1995; Hippolyte et al., 2006, 2009, 2012; Gutiérrez et al., 2012 a, b). When combined with recent monitoring data, it is possible to reliably reconstruct slip rates throughout the full history of individual DSGSDs (El Bedoui et al., 2009; Le Roux et al., 2011; Hermanns et al., 2013).

3.2. Methods for short-term (<10^2 years) dynamics of DSGSDs

Requirements for DSGSD monitoring sensors and data processing differ significantly from those designed for shallower and faster landslides. Such instruments have to detect movements at rates close to their sensitivity limits over protracted time periods (Klimeš et al., 2012). Recent technologies (e.g. in SafeLand deliverable 4.1, 2010) provide wide range of mechanical, electrical, optical and microwave sensors, both ground based and space borne along with advanced processing techniques which are suitable for DSGSDs monitoring. The main development in the last decades includes techniques with millimeter to sub-millimeter precision, and/or semi-continuous data readings, or wide aerial coverage (Table 2). These technologies allow for reliable and detailed correlations between DSGSD movements and changes of triggering factors such as earthquakes or pore water pressure.

Point based measurements most often only detect changes in distance between two fixed points, usually through geodetic techniques (e.g. EDM — Electronic Distance Meter, Berardino et al., 2003; Rizzo and Leggeri, 2004; Brückl and Parotidis, 2005; Crosta et al., 2014) or

Table 2
Major methods and instruments for estimation and measurements of short-term movements of DSGSDs. The technical details for short-term ($<10^2$ years) movement detection technologies are taken from SafeLand deliverable 4.1 (2010) and Klimeš et al. (2012).

Monitoring method	Requirements	Potentials	Limitations	References of the most important studies
Space born Synthetic Aperture Radar (SAR) interferometry: PS-SAR, DInSAR, SqeeSAR	• Suitable land surface conditions (e.g. snow/ice free)	• Capable of providing precise movement data for wide areas • Precision in movement detection in the range of 10^1–10^{-1} mm	• Coarse data re-acquisition periods • Movement detection constrained by the geometry of the satellite's line of sight	Berardino et al. (2003) Delacourt et al. (2007) Tamburini et al. (2011); Tolomei et al. (2013)
Ground-based differential interferometry	• Direct visibility of the DSGSD features from the acquisition point and suitable land surface conditions	• Large detection range (e.g. over 2 km) • High spatial resolution (<1 m) • Almost independent from weather conditions • Precision of 10^{-1} mm • Semi-continuous data acquisition intervals (<1 h)	• Covers relatively small areas	SafeLand deliverable 4.1 (2010) Barla et al. (2010)
Inclinometers and or multi-parametric borehole probe (DMS)	• Have to cross strata of the main deformation activity • Highly sensitive to proper location selection	• Movement detection in 2D or 3D below ground; in the case of DMS, it provides readings of other relevant parameters (e.g. piezometric water levels, movement accelerations)	• Relatively expensive technology requiring drilling and expensive instruments	Bonci et al. (2010), Crosta et al. (2014)
GPS, GNSS	• Direct satellite visibility	• Provides movement vectors and changes of absolute position • Enables semi-continuous data acquisition • Improved precision also allows reliable detection of vertical movements.	• Satellite visibility may be obscured by topography or forest cover.	Booth et al. (2014); Barla et al. (2010); Bonci et al. (2010); Moro et al. (2007)
Geodetic measurements	• Well stabilized monitoring points allowing repeatability over prolonged time periods	• Relatively fast detection of movements of number of monitoring points • Relatively inexpensive and simple technology	• Provides only 1D or 2D relative measurements • Longer data acquisition intervals (days or more), unless an Electronic Distance Meter (EDM) is applied	Rizzo and Leggeri (2004); Brückl and Parotidis (2005); Barla et al. (2010); Le Roux et al. (2011); Crosta et al. (2014)
Distometers, extensometers	• Identification of accessible cracks or near surface discontinuities, which reflect the dynamics of deep-seated movements	• Good precision 10^{-1}–10^{-3} mm • Continuous data acquisition	• Records only relative distance changes, which are sometimes difficult to interpret	Le Roux et al. (2011); Barla et al. (2010); Crosta and Agliardi (2002); Berardino et al. (2003)

extensometers equipped with various sensors (e.g. vibrating wire displacement transducers, Barla et al., 2010; fiber optical interferometers, Woschitz and Brunner, 2008). Geodetic nets or combination of several extensometers are needed for determining displacement vectors. The Global Positioning System (GPS, Moro et al., 2007; Barla et al., 2010; Bonci et al., 2010) or Global Navigation Satellite System (GNSS, Booth et al., 2014) directly measure such displacement vectors, although only recently did this approach achieve satisfactory vertical precision. Optical–mechanical crack gauges designed for long-term, slow-moving landslide monitoring are an alternative, providing three-dimensional data on deformations of "$<10^{-2}$ mm" (Klimeš et al., 2012). Such gauges also detect rotation in two perpendicular planes that in some cases have proved to be highly sensitive to rock deformations (Hasler et al., 2012). Inclinometers or multi-parametric borehole probes (DMS) placed at sufficient depths provide vertically differentiated and spatially oriented information regarding subsurface movements (e.g. Crosta et al., 2014).

Another group of monitoring techniques provides spatial information about movement of the entire or large, continuous body of a given DSGSD. Synthetic Aperture Radar (SAR) interferometry is a popular method for quantifying movement rates and mapping deforming areas that may be otherwise difficult to identify (Tolomei et al., 2013). Spaceborne as well as ground-based SAR sensors can operate over long distance ranges (e.g. up to 3 km, SafeLand deliverable 4.1, 2010) in almost any weather and ground conditions, except for snow-covered terrain. This is an advantage relative to other sensors with large spatial coverage (e.g. satellite images, laser scanners). Improving data processing algorithms for SAR (e.g. Berardino et al., 2003, Delacourt et al., 2007) and the use of permanent scatterers that provide stable radar reflections (Ambrosi and Crosta, 2006) allow millimeter-scale precision in detecting displacement within large areas (Tamburini et al., 2011).

Despite these recent advances in monitoring techniques, several data acquisition drawbacks make it difficult to obtain long-term, reliable, and easily interpreted information about DSGSD activity. A common drawback is incomplete time-series data caused by technical reasons such as equipment failures or instability of measured targets (Rizzo and Leggeri, 2004; Vilímek et al., 2007). In addition, the latter is rarely discussed or evaluated in detail, despite evidence that it may significantly affect measurement results (Lambiel and Delaloye, 2004). Homogenous coverage of the entire, usually large bodies of DSGSDs, with equally precise and frequent monitoring data is rarely achieved as the majority of the monitoring methods are point based. Radar remote sensing largely overcome this obstacle, but reliable results are usually available only for part of the raw datasets (e.g. Berardino et al., 2003; Moro et al., 2009), and the best aerial coverage is in regions with only sparse vegetation cover (e.g. Newman, 2013). Interpretation of the results is further hindered by a low intercomparability between different monitoring techniques due to varying precision, measurement frequency, and spatial coverage. Barla et al. (2010) showed that results of manual and automated geodetic measurements of the same targets may provide slightly different movement vectors.

4. Evolution of DSGSDs on ≥10^2-year time scales

DSGSDs are long-lasting features with complex and often changing displacement dynamics (McCalpin and Irvine, 1995; Tibaldi et al., 2004; Baroň et al., 2013). Recent research in tectonically active mountain belts show that DSGSDs play an important role as denudation agents both at the hillslope (Korup, 2006) and orogen scale (Agliardi et al., 2013), thus contributing to the longer-term evolution of mountains. Despite remaining an open question, our knowledge about the long-term dynamics of DSGSDs has made great strides over the last two decades thanks to better constraints on the life spans of DSGSDs and refined data on the regimes of associated displacement rates.

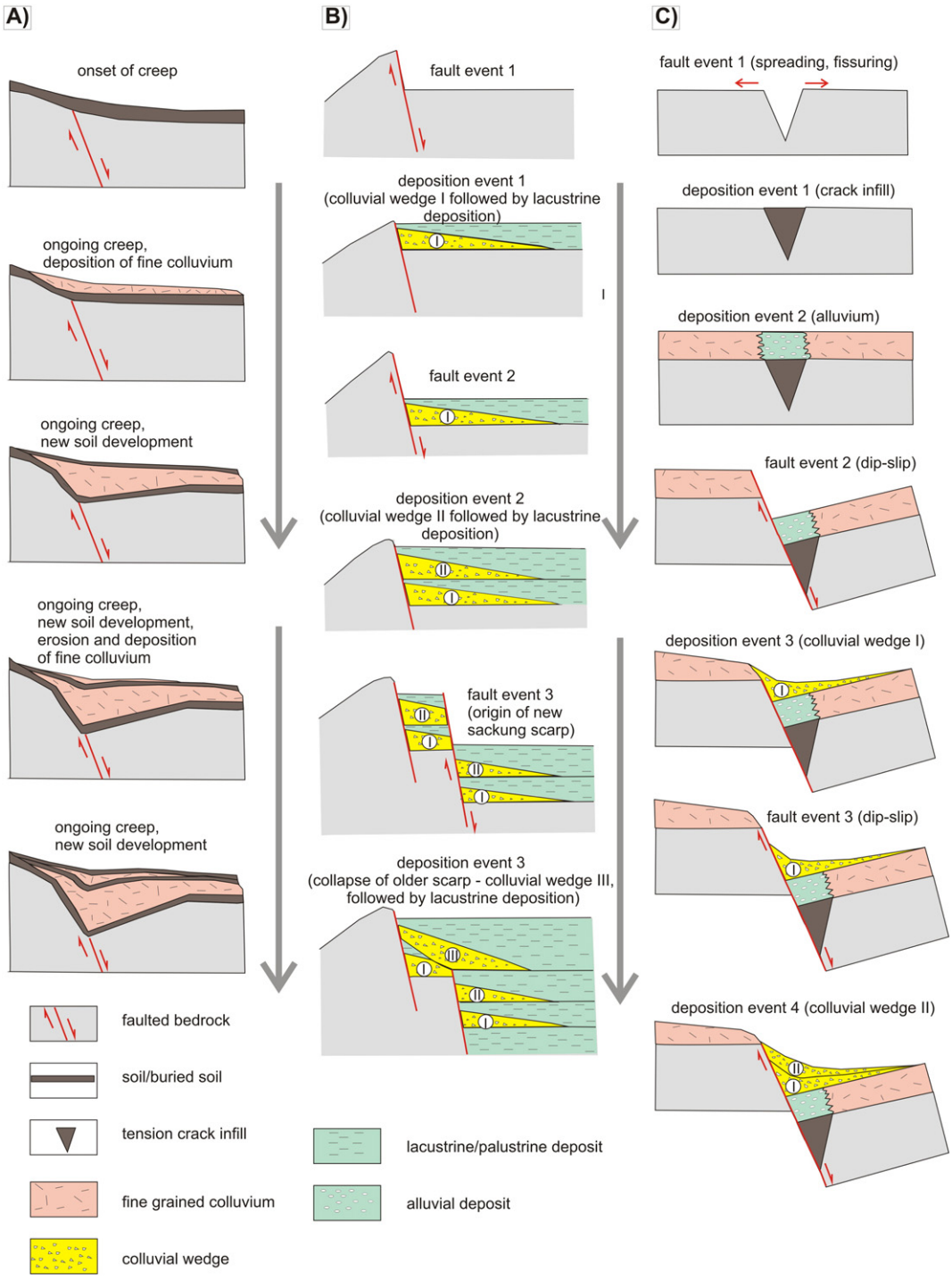

Fig. 3. Some common structures and deposits observed within paleoseismic trenches applied across DSGSDs scarps. Event-response sequences leading to particular structural–depositional patterns (lowermost sections) associated with three distinct types of DSGSDs movements are depicted. A. Sackung faults experiencing continuous, creep-type movements (herein decelerating in time) with prevailing ductile deformation of deposits. A prominent characteristic feature is the absence of colluvial wedges (e.g. McCalpin and Irvine, 1995). B. Episodic dip-slip movements on sackung faults (herein with progressively increasing offset) with related colluvial wedges and lacustrine/palustrine deposits revealing stages of inactivity (the case presented by Gutiérrez et al., 2008). C. Complex deformation pattern characteristics by alteration of spreading (formation of tension cracks) and dip-slip movements with associated colluvial wedges (simplified case of Blue Ridge sackung published by McCalpin and Hart, 2003).

4.1. The lifespan of DSGSDs

Geological evidence from speleothems, calcite veins infilling tension cracks (Pánek et al., 2009b; Urban et al., 2013) or zeolite growth in fractured rocks moved by DSGSDs (Bovis, 1982) reveal that such deformation may evolve over $>10^4$–10^5 years. Yet any morphologic legacy is often overprinted by glaciation, fluvial erosion or catastrophic collapses. Thus, recent morphologic expression relates only to the youngest generations of DSGSDs. Additionally, determining the onset of a given DSGSD is limited by the short time-range of suitable absolute dating techniques (Walker, 2005). Often, our knowledge regarding particular DSGSDs only includes their minimum lifespans (Fig. 4A, Table 3). A growing number of absolute dated DSGSDs (Fig. 1) allows distinguishing two main types with different lifespans, i.e. (i) those situated in formerly glaciated terrain with an onset of activity mainly occurring after ~18–10 ka when final deglaciation occurred in most mountain

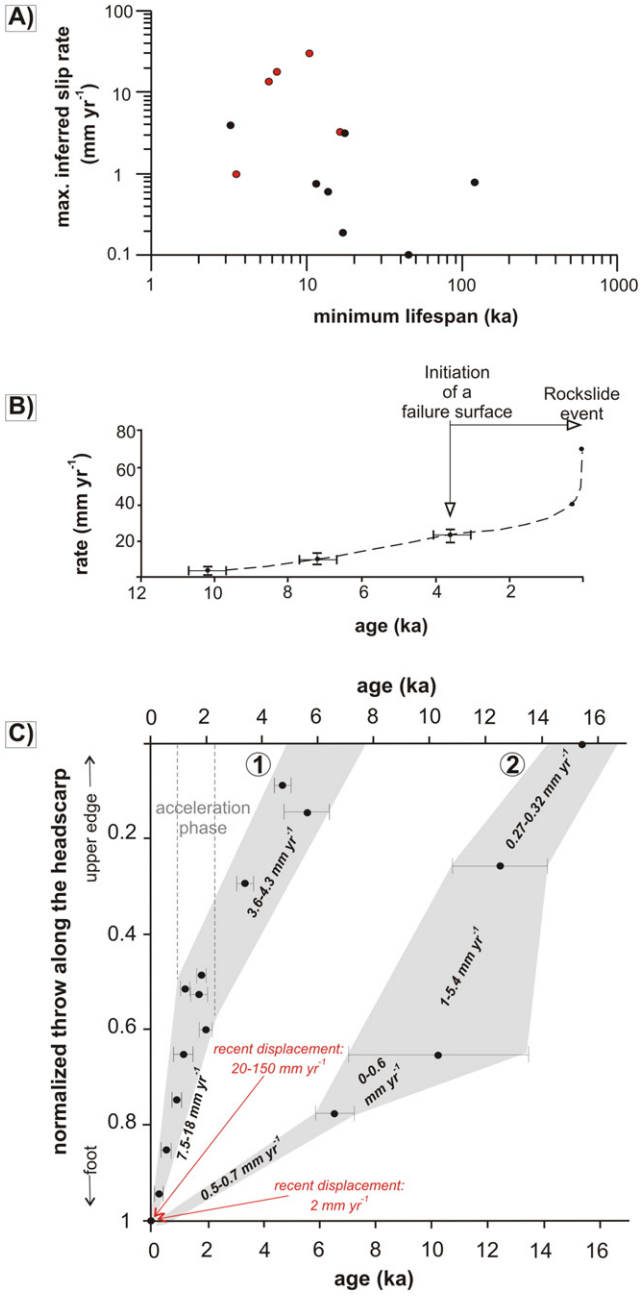

Fig. 4. Long-term displacement trends of some DSGSDs and DSLs. A. Maximum inferred rates of dated DSGSDs (DSLs are represented by red dots) plotted against their minimum lifespan. B. Long-term horizontal movements and opening of tensile cracks within the La Clapière sackung (French Alps) transformed in the mid-Holocene to predominantly vertical, accelerating shearing, which led to the formation of a distinct landslide body in the last 50 years (El Bedoui et al., 2009). C. Vertical displacements of selected DSLs where TCN dating is supplemented by the monitoring of recent movement; indicated by the throw along the headscarp. 1 — An example of a DSL that accelerated slip rates during the late Holocene (Séchilienne/French Alps; Le Roux et al., 2009), 2 — Long-term diminishing slip rates inferred for the Oppstadhornet deep-seated rockslide (Otrøya Island/Norway; Hermanns et al., 2013).

belts (Hughes et al., 2013); and (ii) those evolving in non-glaciated settings with a generally longer and more complex chronology, often predating global Last Glacial Maximum (~23–19 ka; Hughes et al., 2013). The age distributions of both distinct groups using the hitherto published ages of DSGSDs and DSLs in previously glaciated and non-glaciated mountains are presented in Fig. 5.

Examples for the first group come from the highest and/or high-latitude mountain belts, such as the Rocky Mountains (McCalpin and Irvine, 1995), Alaska (McCalpin et al., 2011), Iceland (Coquin et al., 2015), Scandinavian Mountains (Hermanns et al., 2013), European Alps (Hippolyte et al., 2006, 2009, 2012; Agliardi et al., 2009a; Le Roux et al., 2009), and the Pyrenees (Gutiérrez-Santolalla et al., 2005; Gutiérrez et al., 2008) (Table 2). Although some of these DSGSDs originated just after Pleistocene ice masses retreated (e.g., Hippolyte et al., 2012), most of them probably experienced a substantial time lag (~2–6 ka) following glacial withdrawal. The complex responses of rock slopes, potentially related to stress relaxation, subcritical crack growth, and the progressive failure of intact rock bridges could cause such delay (Kemeny, 2003; McColl, 2012; Ballantyne et al., 2014). For example, the sackung that affected the Aspen Highlands in the Rocky Mountains (Colorado, USA) originated 2.5–4 ka after deglaciation (McCalpin and Irvine, 1995). However, some examples from the European Alps reveal even more pronounced delays relative to ice retreat, reaching ~6.5–9.5 ka (Le Roux et al., 2009; Sanchez et al., 2010). Although glacier activity during the Last Glacial period may have obliterated most DSGSD-related landforms, some deformations seem to have survived repeated glacial advances. Based on trenching, Tibaldi et al. (2004) stated that the DSGSDs on the western bank of the Lago Maggiore (Italian Alps) began during the last interglacial period (~120 ka BP) and had several reactivations, including reactivations during the post-glacial period. The possibility of a continued evolution of DSGSDs partially or fully covered by glaciers remains a challenging question. Some have suggested (Turnbull and Davies, 2006; McColl and Davies, 2013) that DSGSDs may move into glaciers well before the onset of deglaciation due to the higher densities of the rocks relative to the density of glacier ice.

The morphological legacy of DSGSDs and DSLs in non-glaciated regions is often much longer, usually more than 30–40 ka (Pánek et al., 2009b; Gutiérrez et al., 2012b; Baroň et al., 2013; Gori et al., 2014) (Fig. 5, Table 3). An exception is given by areas with mechanically weak and easily erodible rocks such as flysch, where the age of DSGSDs and DSLs rarely exceeds the Late Glacial (Margielewski, 2006; Pánek et al., 2011a). Using a combination of ^{14}C and OSL dating, Baroň et al. (2013) reconstructed a ~42-ka-long history of deep-seated failures and associated shallower mass movements for the giant (83–110 km^3) Quoshadagh slope deformation in NW Iran. Similar lifespans were reported for some DSGSDs in the foothills of the Pyrenees (>45 ka; Gutiérrez et al., 2012b) and the Central Apennines (~44 ka; Gori et al., 2014). While the true ages of some of the DSGSDs in such settings appear to be much older, potentially spanning the entire Quaternary period (Esposito et al., 2013; Gori et al., 2014), such a notion awaits confirmation by absolute dating. Some of the oldest dates from DSGSDs from geochronological data were obtained from karst areas underlain by carbonate rocks. Based on the $^{230}Th/^{234}U$ dating of speleothems covering the walls of exposed limestone scarps and cracks, a >100 ka history of slope deformation characterizes the large-scale spreading that affected the margins of the karst plateau in the Crimean Mountains/Ukraine (Pánek et al., 2009b; Fig. 6). Zerathe and Lebourg (2012) demonstrated that the deep-seated landslide in the Maritime Alps (France) is older than the overlying calcareous tufa, which was constrained by uranium-series dating to >400 ka.

4.2. Long-term deformation trends

The growing information about the timing of DSGSDs generally reveals two basic long-term movement patterns of DSGSDs, i.e. slow continuous creep (McCalpin and Irvine, 1995; El Bedoui et al., 2009; McCalpin et al., 2011; Hermanns et al., 2013); and discrete episodic movements (McCalpin and Hart, 2003; Tibaldi et al., 2004; Gutiérrez-Santolalla et al., 2005; Gutiérrez et al., 2008, 2012a, b; Agliardi et al., 2009a; Moro et al., 2012; Carbonel et al., 2013; Gori et al., 2014; Table 3). These two types of movements were expected for DSGSDs long before the first dating and monitoring studies (Němčok, 1972; Radbruch-Hall, 1978). Both types are contrasting end

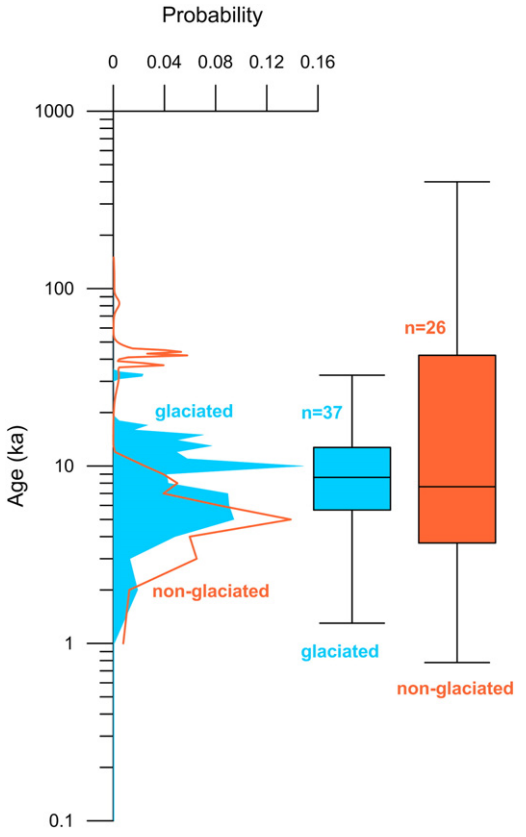

Fig. 5. Probability distributions and variability of ages expressed as box-whisker plots for published DSGSDs and DSLs situated in formerly glaciated terrains and in non-glaciated settings.

members of possible DSGSDs histories in the much broader spectrum of transitional displacement types involving alternating phases of sudden acceleration or catastrophic failure and long-term creep deformation (Fig. 3). Some studies have revealed that both creep and episodic movements can operate in constant (Hippolyte et al., 2012), accelerating (e.g. Gutiérrez et al., 2008) or decelerating (e.g. McCalpin and Irvine, 1995) modes over long ($\geq 10^2$ years) time spans. As displayed in Fig. 3C, some paleoseismologic trenches even reveal long-term changes in DSGSD kinematics. For example, lateral spreading is replaced after some time by dip-slip movements typical of sliding or sagging (McCalpin and Hart, 2003). Inferred long-term slip rates of individual DSGSDs range from ~0.1 (Gutiérrez et al., 2012b) to 5 mm year^{-1}; whereas DSLs usually exceed 15 mm year^{-1} reaching up to 80 mm year^{-1} (El Bedoui et al., 2009; Fig. 4A; Table 3).

Creep-type displacements were documented for DSGSDs that originated from Late Glacial ice retreat and hillslope debutressing (McCalpin and Irvine, 1995; Hippolyte et al., 2009). McCalpin and Irvine (1995) concluded that a trenched sackung scarp in the southern Rocky Mountains experienced a 75% decrease in deformation rates between ~11.5 and 7 ka, i.e. a few thousand years after deglaciation started. Similarly, Hippolyte et al. (2006; 2009) reported that DSGSDs in the French Alps terminated their movement after only a few thousand years following deglaciation and stressed that the long-term deformation of DSGSDs is largely related to their kinematics and the thickness of deformed rock mass (Hippolyte et al., 2006, 2009). El Bedoui et al. (2009) described contrasting types of creeping postglacial DSGSDs in the French Maritime Alps (La Clapière slope) where initial slow postglacial movements (~4 mm year^{-1}) accelerated throughout the Holocene and where progressive lowering of rock strength led to the formation of a distinct landslide body with movements of >80 mm year^{-1} (Fig. 4B; El Bedoui et al., 2009; Lebourg et al., 2011). Similar long-term creeping movements, predominantly one order higher than those typical of DSGSDs, have recently been inferred by TCN dating and monitoring in the case of Séchilienne (Le Roux et al., 2009) and Oppstadhornet (Hermanns et al., 2013) DSLs, suggesting distinctions between the dynamics of DSGSDs and DSLs (Fig. 4C).

Episodic displacements, mostly with millennial recurrence intervals (e.g., Gutiérrez et al., 2008; 2012a, b) characterize DSGSDs exposed to active seismicity near major faults (Thompson et al., 1997; McCalpin and Hart, 2003; Gutiérrez et al., 2008) or directly superimposed on active fault scarps or horsts (McCalpin et al., 2011; Moro et al., 2012; Gori et al., 2014). Some reactivations of sackung movements were correlated with paleoseismic evidence (Moro et al., 2012). A few dated

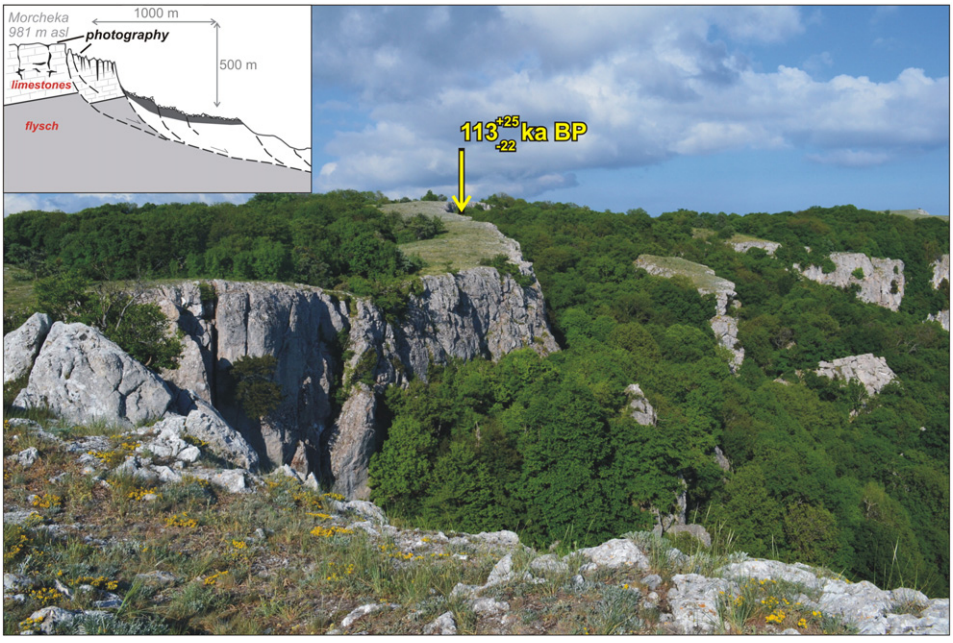

Fig. 6. Large-scale spreading affecting Jurassic limestones at the margin of the karst plateau in the SW portion of the Crimean Mountains (Ukraine). $^{230}Th/^{234}U$ dating of the basal layers of speleothems covering sub-vertical scarps within the DSGSD indicates that tension cracks began to widen at >100 ka BP. The position and results of dating are indicated by the arrow.

Table 3
Time span and dynamics of DSGSDs hitherto constrained by absolute dating, n.a. — not ascertained.

DSGSD (DSL*, DSL within DSGSD**) location/region	Age (ka)	Inferred slip rates (mm year^{-1})	Glaciated in the Last Glacial period (Y/N)	Type of movements — episodic (E) or continuous (C) /comment	Dating method used	References
La Marbrière/Maritime Alps (France)*	>400	n.a.	N	n.a./lateral spreading + toppling, part of the slope collapsed before ~3.9 ± 0.2 ka	Uranium-series, ^{36}Cl, ^{10}Be	Zerathe and Lebourg (2012); Zerathe et al. (2014)
Mt. Scincina/Italian Alps	>120	0.5–0.8	Y	E/sackung-type movements, survived successive glaciations	^{14}C, OSL + relative dating	Tibaldi et al. (2004)
Foros/Crimean Mountains (Ukraine)	>110	n.a.	N	n.a./lateral spreading + toppling, accompanied by younger collapse	Uranium-series, ^{14}C	Pánek et al. (2009b)
Perecalç/Spanish Pyrenees	>45	>0.1	N	E/lateral spreading due to interstratal dissolution of evaporites	^{14}C, OSL	Gutiérrez et al. (2012b)
Mt. Quoshadagh/Iran	>42	n.a.	N	n.a./close to active transpressive fault, DSGSD accompanied by shallower mass movements	^{14}C, OSL	Baroň et al. (2013)
Mt. Morrone/Apennines (Italy)	>41	n.a.	N	E + C/sackung in the vicinity of seismogenic fault, accompanied by younger collapses	^{14}C	Gori et al. (2014)
Bregaglia Valley/Swiss + Italian Alps	>29–16	n.a.	Y	n.a./sackung probably driven by river capture, close to the seismogenic Engadin Fault	^{14}C, OSL + relative dating	Tibaldi and Pasquarè (2008)
Mt. Rognier/French Alps	~17	0.29–3.15	Y	C(?)/ongoing sackung activity driven likely by seismicity and/or interstratal dissolution of evaporites	^{10}Be	Hippolyte et al. (2012)
Oppstadhornet/Norway*	~16.6–14.2	0.6–3.2	Y	C/recently monitored by GNSS — ongoing slip at ~2 mm year^{-1}	^{10}Be	Hermanns et al. (2013)
El Ubago/Spanish Pyrenees	~16.9	>0.19	Y	E/sackung likely driven by seismicity, recurrence interval of dip-slip movements ~5.6 ka	^{14}C	Gutiérrez et al. (2008)
Zenzano Fault/Iberian Chain (Spain)	>13.6	0.6	N	E/sackung due to interstratal dissolution of evaporites, recurrence interval ~3.2–6.7 ka	^{14}C	Carbonel et al. (2013)
Aspen Highlands/Colorado (USA)	~11.5–11	0.14–0.75	Y	C/dip-slip, alt. Toppling kinematics accomplished by horizontal spreading at 0.43 mm year^{-1} in the past 3 ka	^{14}C	McCalpin and Irvine (1995)
Arcs/French Alps	~11.5	n.a.	Y	C(?)/flexural toppling, rapidly originated in few millennia between ~11.5–8.5 ka	^{10}Be	Hippolyte et al. (2009)
Kagel Mountain/San Gabriel Mts. (California, USA)	~10.7	n.a.	N	E/sackung activity likely driven by adjacent seismogenic San Gabriel fault	^{14}C	McCalpin and Hart (2003)
La Clapière/French Alps**	10.3	4–30	Y	C(?)/multiply monitoring reveal ongoing accelerated slip exceeding 80 mm year^{-1}	^{10}Be	Bigot-Cormier et al. (2005); El Bedoui et al. (2009)
Mt. Kushtaka/Yakutat microplate (Alaska, USA)	>10.2	n.a.	Y	C/flexural toppling, beginning of the activity just after deglaciation	^{14}C, OSL	McCalpin et al. (2011)
Mt. Watles/Italian Alps	~10	n.a.	Y	E/at least four episodic events during the Holocene	^{14}C	Agliardi et al. (2009a)
Mt. Serrone/Apennines (Italy)	~9.6	n.a.	N	E and C/sackung likely driven by nearby seismogenic fault/ongoing activity revealed by InSAR measurements	^{14}C	Moro et al. (2012)
Vallibierna and Estós sackungen/Spanish Pyrenees	~7.8–5.9	n.a.	Y	E/beginning >5 ka after deglaciation, driven likely by seismic activity	^{14}C	Gutiérrez-Santolalla et al. (2005)
Séchilienne/French Alps*	6.4	3.6–18	Y	C/originated during humid Holocene Climatic Optimum, monitoring reveal ongoing slip at ~13 mm year^{-1}	^{10}Be	Le Roux et al. (2009)
Mt. Ondřejník/Western Carpathians (Czech Republic)	>5.9	n.a.	N	E(?)/lateral spreading, accompanied by shallower mass movements	OSL	Pánek et al. (2011a)
Le Pra/French Alps**	5.7	0.7–13.5	Y	C(?)/deep-seated landslide	^{10}Be	Sanchez et al. (2010)
Blue Ridge and Lytle Creek sackungen/San Gabriel Mts. (California, USA)	4.2–0.8	n.a.	N	E/sackung activity likely driven by adjacent seismogenic San Andreas fault	^{14}C	McCalpin and Hart (2003)
Teruel Graben/Iberian Chain (Spain)	3.5	0.6–1	N	E/sackung due to interstratal dissolution of evaporites, recurrence interval ~1.2–2 ka	^{14}C	Gutiérrez et al. (2012a)
Caire/Maritime Alps (France)*	>3.2	1.6–4	N	C/deep-seated translational landslide combined with lateral spreading	^{36}Cl	Zerathe et al. (2014)
Affliction Creek/Coast Mountains (British Columbia, Canada)	Onset of activity between AD 1865–1875	n.a.	Y	C(?)/flexural toppling with retrogressive behavior	lichenometry	Bovis (1982)

seismically induced sackungen shows that each successive earthquake event produces an increasing amount of deformation, perhaps reflecting the progressive weakening of the rock mass strength (Gutiérrez et al., 2008). Clearly, a more extensive database of dated DSGSDs in seismically active areas is needed to determine whether this behavior is widespread or site-specific. In addition to earthquakes, highly episodic displacements have recently been reported for some DSGSDs in the Pyrenees and Iberian Range (Spain), caused by subsidence due to the interstratal dissolution of evaporites (Gutiérrez et al., 2012a, b; Carbonel et al., 2013). Although dissolution is a continuous process, collapses only occurred when the volume of void space reached a critical value and the stability threshold of the overlying rocks was exceeded (Gutiérrez et al., 2012a, b). Because dissolution is clearly related to the amount of precipitation and groundwater recharge,

Table 4
Overview of the monitored DSGSDs reveals short-term displacement behavior. Abbreviations: PS-SAR — Permanent Scatter Synthetic Aperture Radar; SBAS DInSAR — Small Baseline Subset multi-temporal Differential Synthetic Aperture Radar Interferometry; GB-InSAR — Ground Based-Synthetic Aperture Radar Interferometry; EDM — Electronic Distance Meter; dGNSS — differential Global Navigation Satellite System; dGPS — differential Global Positioning System; ? — calculated using figures from the articles; deform. — deformation; SC — slope creep; IA —irregular acceleration; RA — regular acceleration; n.a. — not ascertained. If not otherwise indicated, movement rates represent horizontal displacement.

Location	Depth (m)	Monitoring technique	Monitoring period	Data reading intervals	Maximum movement rates (mm year^{-1})	Average annual movement rates (mm year^{-1})	Period of increased activity	Factors causing increased activity	Short-term deform. pattern	Comment	References
Parohy, Carpathians, Slovakia	>100?	Optical crack gauge	1973–2010	1 month	1?	0.07	Spring	n.a.	IA	Sackung monitoring	Briestenský et al. (2011)
Taukliman, Bulgarian coast	>50?	Optical crack gauge	1973–1992	1 month	5?	1.2?	April 1977, August 1986, May 1990	Earthquakes, rainfalls	RA and IA	Lateral spread monitoring	Košťák (1981); Klimeš et al. (2012)
Maratea, South Italy	100?	EDM	1983–1999	n.a.	24	7–24	Since 1991	Tectonic movements	IA	Sackung and lateral spread monitoring	Rizzo and Leggeri (2004)
Mt. Legnoncino, Italian Alps	n.a.	PS-SAR	1991–2002	n.a.	20	2–20	November 2000	Extreme rainfalls	IA	Sackung monitoring	Ambrosi and Crosta(2006)
Cyrilka, Carpathians, Czech Rep.	>50	Optical crack gauge	2001–2011	1 month	0.2?	0.02	Autumn	Rainfalls	RA	Lateral spread monitoring	Klimeš et al. (2012)
Greci, South Italy	70	GPS(1), Inclinometers (2)	1996–2006	1 year (1)	5 (1)	5 (2)	n.a.	n.a.	n.a.	Sackung monitoring	Bonci et al. (2010)
Fucion Basin, Apenines, Italy	600	DInSAR	1992–2001	3 months	4.5	0.5–4	Beginning of 1998	Extreme rainfalls	IA	Lateral spread monitoring	Moro et al. (2009)
Mt. Padrio–Mt. Varadega, Italian Alps	n.a.	PS-SAR	1992–2003	n.a.	n.a.	1–3?	n.a.	n.a.	n.a.	Sackung monitoring	Ambrosi and Crosta(2006)
Beauregard, Italian Alps	>147	Geodetic survey, GPS(1), GB-InSAR (5)	2000–2007 (1); 2008	1 year (1); 20 min (5)	2.4	1.4 (1)	Spring/summer	Snow melt, rainfalls	RA	DSGSD monitoring	Barla et al. (2010)
Podall, Apenines, Italy	500–600	DInSAR	1993–2000	3 months	100 (vertical movement)	30–40 (vertical movement)	November 1999	Extreme rainfalls, earthquakes	IA	Sackung monitoring	Tolomei et al. (2013)
Lesachriegel, Austrian Alps	n.a.	Geodetic survey	1972–1976	n.a.	3000 mm in single event	10	1965	Extreme rainfalls	IA	Sackung monitoring	Brückl and Parotidis (2005)
Colfiorito, Apenines, Italy	200	DInSAR	September–October 1997	n.a.	80 mm during single event	n.a.	September 1997	Earthquake ($M_w = 6$)	IA	Sackung monitoring	Moro et al. (2007)

DSGSD development is more intense during humid climatic phases (Gutiérrez et al., 2012b).

5. Evolution of DSGSDs on $<10^2$-year time scales

Creeping slopes have for a long time been recognized as hazards to construction and operation of important infrastructure such as dams, roads, and mining facilities (Záruba and Mencl, 1969). The first measurements of the movement of DSGSDs used geodetic techniques (Hauswirth et al., 1979), and attempted to control deformed slopes interfering with dam construction sites (Novosad, 1956, 1966, 2002; Barla et al., 2010). New monitoring methods (e.g. Moser et al., 2002), collection of decades-long time-series of movements, and techniques allowing high data acquisition frequencies and dense spatial coverage now enable reconstruction of more complex DSGSD behavior (Table 4).

5.1. First-time occurrences of DSGSDs

Very few case studies describe the first-time occurrences of DSGSDs such as emergence of entirely new scarps and other morpho-structures (Bovis, 1982; Carton et al., 1987; Evans and Clague, 1993; Blair, 1994; Dramis and Sorriso-Valvo, 1994; Jibson et al., 2004; Brückl and Parotidis, 2005). These cases are exclusively related to strong earthquakes, heavy rainfall or deglaciation following the Little Ice Age. A more recent example concerns sackungen that formed during the Denali fault earthquake in 2002 (Jibson et al., 2004). In this case, a deformation of up to 1500 m wide, with individual counter-slope scarps that were up to 5-m high occurred on previously undisturbed ridges during the M_w 7.9 earthquake (Fig. 2D). Other examples include multiple scarps and grabens that originated due to the deep-seated gravitational movements of Pleistocene conglomerates overlying Miocene marls

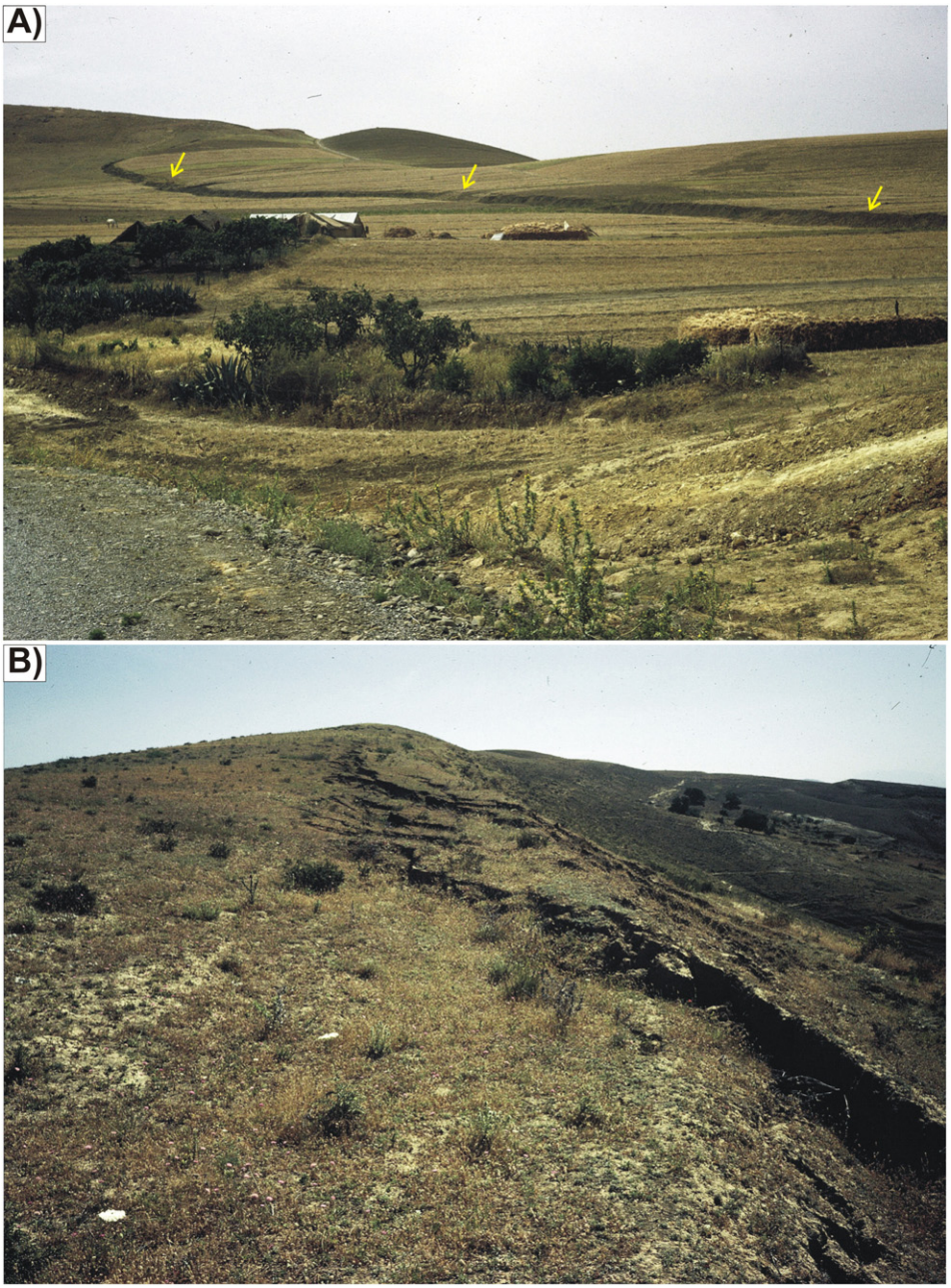

Fig. 7. Newly formed scarps (up to 2 m high) related to deep-seated gravitational movements, which accompanied the M_w 7.3 1980 El Asnam earthquake in Algeria. A. Part of the arc-shaped scarp (marked by yellow arrows) originated as a gravitational adjustment driven by seismic shaking and gravitational gradient toward the adjacent Oued Cheliff gorge. B. Uppermost scarp parallel to the main seismogenic thrust fault in Serat-el-Maarouf site (photo courtesy: M. Sorriso-Valvo).

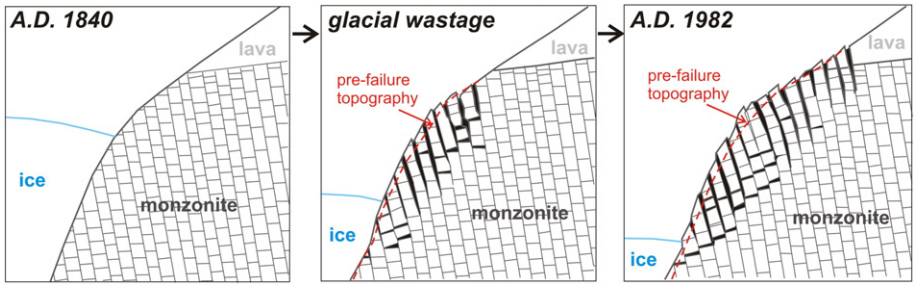

Fig. 8. Schematic expression of the flexural toppling retrogressive shift after glacier thinning following the LIA culmination (AD ~1840) in the Coast Mountains (British Columbia, Canada; adopted from Bovis, 1982).

around the epicenter of the 1980 M_w 7.3 El Asnam earthquake in Algeria (Fig. 7; Carton et al., 1987; Dramis and Sorriso-Valvo, 1994). Some rare observations of the abrupt formation of DSGSDs following recent deglaciation have been presented. Contemporary development of uphill-facing scarps as a response to post-Little Ice Age glacial thinning was reported in British Columbia (Fig. 8; Bovis, 1982; Evans and Clague, 1993), and New Zealand (Blair, 1994). Even more scarce observations are related to rainfall-induced sudden activations of DSGSDs. Brückl and Parotidis (2005) describe an example of the Lesachriegel sackung in Austrian Alps where a 3-m-slip on sackung scarp took place in 1965 as a consequence of heavy rainfall.

5.2. Short-term deformation trends

Monitoring results provide a base for defining several temporal movement patterns of DSGSDs with variations at annual and decadal scales. Slope creep is the main movement type. It is steady displacement maintaining the same movement rate without clear acceleration phases. Nevertheless, the steady displacement is often interrupted by regularly or irregularly distributed movement accelerations related to seasonal climatic variations (e.g. increased precipitation possibly combined with snowmelt) or irregularly occurring extreme triggering events (e.g. earthquakes or extreme precipitation, Table 4). Regular accelerations represent continuous seasonal acceleration phases followed by significant decrease in movement rates (Cyrilka and Beauregard in Table 4). On the other hand, irregular accelerations are caused by extreme triggering events preceded and followed by periods of decreased and continuous movement rates. The majority of the monitored DSGSDs exhibit this type of short-term deformation pattern (Table 4). Among the most frequently documented triggers are changes in ground water levels and pore pressures directly linked to the rock deformations (Crosta et al., 2014). Such changes may be caused by short-term, high intensity precipitation (Ambrosi and Crosta, 2006; Brückl and Parotidis, 2005; Moro et al., 2009), cumulative precipitation (Crosta and Agliardi, 2002) or combined with snowmelt (Crosta et al., 2014; Barla et al., 2010). In specific cases, submergence of the toe by a lake may also result into DSGSD movement acceleration (MacFarlane, 2009).

An example of a very slow and steady creep deformation is a sackung of a limestone ridge in the Malá Fatra Mountains, Western Carpathians, Slovakia (Briestenský et al., 2011; Table 3). The average annual vertical movement of this DSGSD over 33 years was 0.07 mm $year^{-1}$ (Fig. 9; Briestenský et al., 2011). Optical–mechanical crack gauge measurements determined that creep affected only vertical component of the main headscarp, while strike-slip and horizontal movements showed only short-term variations without any trend. The complexity of the short-term deformations of this DSGSD is illustrated by three irregularly spaced distinct vertical movement accelerations during spring months (Fig. 9). They were not explained by external factors (e.g. amount of water from snowmelt), and thus probably reflect internal and temporal changes in slope response to the regularly occurring conditions. A different view of short-term deformations of DSGSDs is provided by InSAR interferometry results that cover broad areas but lack detailed 3D perspective (Fig. 10; Moro et al., 2009). Such an analysis offers a valuable insight into the spatial movement pattern that can be related to specific morphological features of DSGSDs as well as temporal changes caused by seismic or hydrological conditions. Seismic shaking related to an M_w 6 earthquake in the Central Apennines was responsible for the acceleration of several DSGSDs affected by up to 80 mm of horizontal displacement (Fig. 10; Moro et al., 2007). Another study shows that repeated co-seismic accelerations of a slowly creeping (0.2 mm $year^{-1}$) lateral spread resulted in horizontal movements (5 mm) that were more than three times larger than the vertical ones (Košťák, 1981; Klimeš et al., 2012).

It is interesting to note that among the published cases there are rarely DSGSDs which express only creep movement during the entire observation period. This is probably because the DSGSDs with accelerated movement phases are morphologically evident and considered to be more hazardous, and therefore are more likely to be monitored.

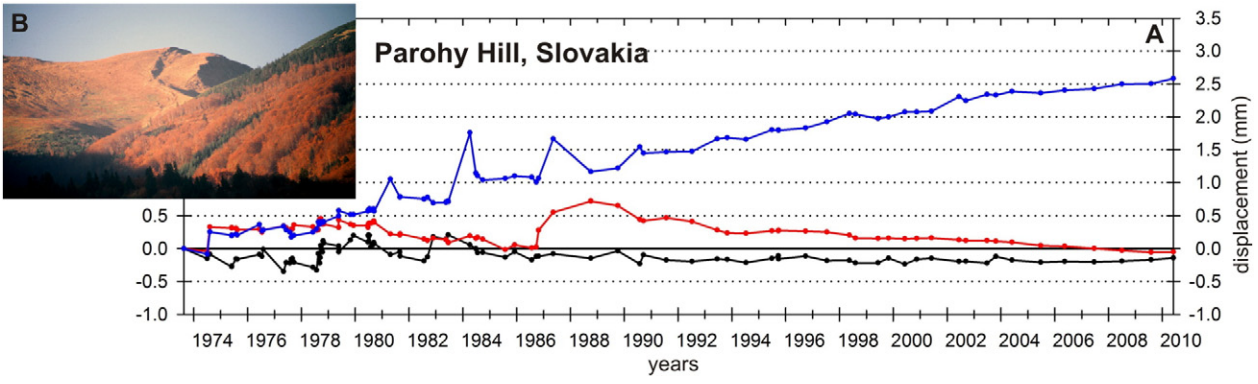

Fig. 9. Results of three dimensional monitorings of movements (A) along headscarp of sackung in Malá Fatra Mts. (Western Carpathians, Parohy Hill, Slovakia). The inset photograph (B) shows headscarp of the DSGSD, blue curve shows vertical displacement, red curve is strike-slip component of the movement and black curve stands for horizontal movements (adapted from Klimeš et al., 2012).

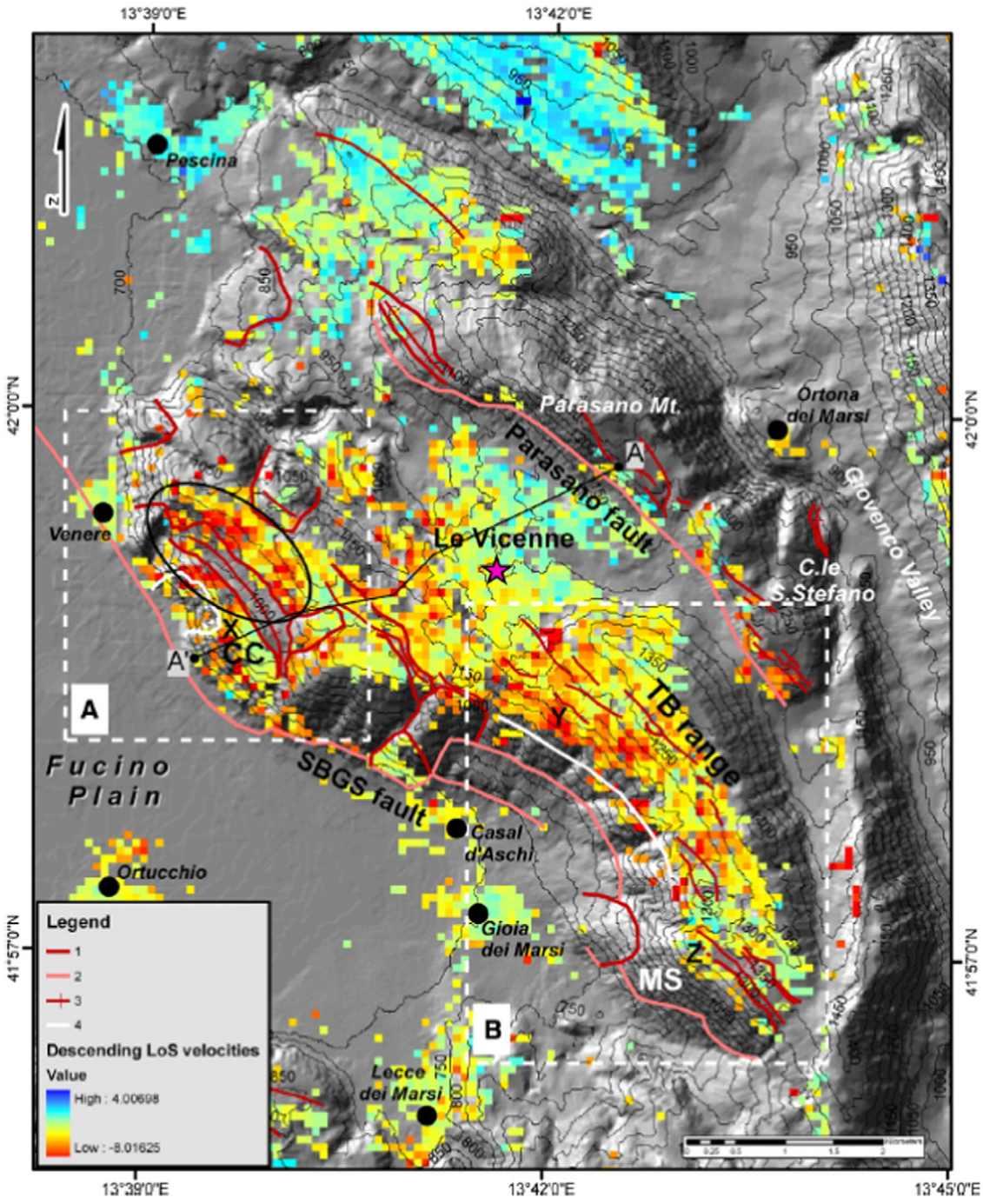

Fig. 10. Results of SBAS DInSAR interferometry of the Fucino Basin DSGSD movements illustrate well the InSAR capability of providing spatially distributed information of movement rates here shown as the Descending Line of Sight (LoS) velocity map (values in mm year^{-1}). Legend: 1) Upper limit of DSGSD; 2) Quaternary active fault; 3) Major trench; 4) Rock avalanche source area. White hatched rectangles define the areas A and B, described in the text. The star represents the reference point for all ground velocities. A–A′ is the trace of the cross-section. Black ellipse represents the lowering NW sector described in the text. Reprinted from Geomorphology, 112, Moro, M., Saroli, M., Tolomei, C., Salvi, S., Insights on the kinematics of deep-seated gravitational slope deformations along the 1915 Avezzano earthquake fault (Central Italy), from time-series DInSAR, 261–276, 2009, with permission from Elsevier.

6. DSGSDs as precursors of catastrophic collapse

Catastrophic failures of sackung slopes as a potential end-member in the evolution of DSGSDs have been subject to many investigations (Bisci et al., 1996; Di Luzio et al., 2004; Chigira, 2009; Chigira et al., 2010, 2013; Nishii et al., 2013; Barth, 2014; Bianchi Fasani et al., 2014). There are two major ways in which prolonged deep-seated gravitational spreading might change stability conditions and make rock slopes more susceptible to catastrophic slope failures: (i) changes of the mechanical properties of rock massif including rock-strength reduction, fragmentation, and tilting of geological structures into unstable positions (Chigira and Kiho, 1994; Bisci et al., 1996; Pánek et al., 2009a; Lebourg et al., 2011 etc.); and (ii) modifications of slope topography, especially over-steepening due to the bulging or buckling and development of new runoff paths (Wilson et al., 2003; Seijmonsbergen et al., 2005; Crosta et al., 2014 etc.; Fig. 11). The main process responsible for these long-term changes is the creep movement characterized by the deformation of rocks under stress (Federico et al., 2012). These rocks are very often localized on discontinuity planes, which results in shearing resistance decrease and consecutive modification in the

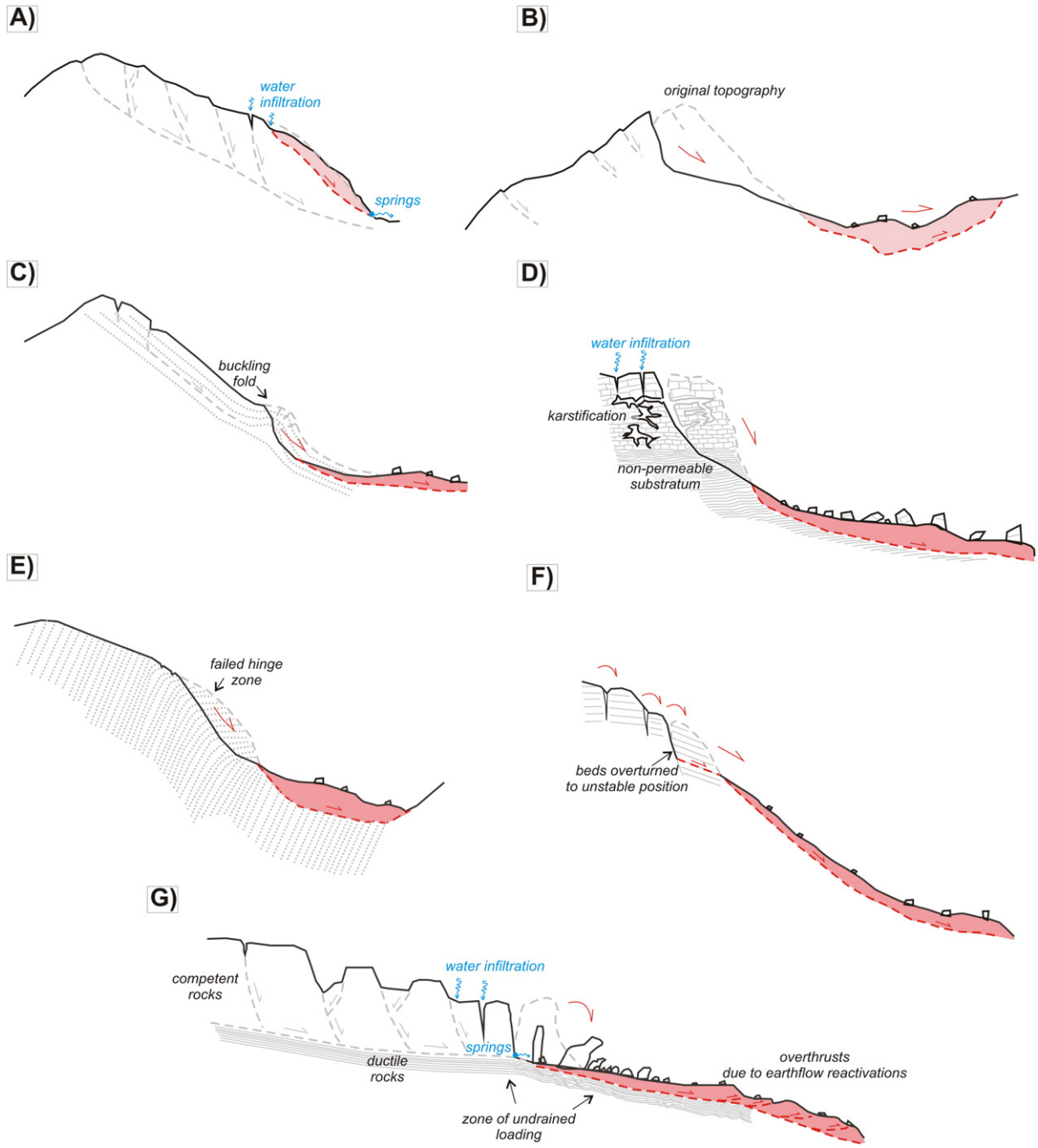

Fig. 11. Possible modes of DSGSD catastrophic failures. A. Landslides originated due to the progressive weakening of bedrock and modification of topography (e.g. slope steepening and the presence of trenches concentrating runoff) in the lower part of DSGSDs (e.g. Crosta et al., 2014). B. Large-scale rock avalanches predisposed by asymmetric sackung faults (e.g. Barth, 2014). C. Rockslides and rock avalanches due to the slope oversteepening and tensile crack development in relation to growth of buckling folds (e.g. Seijmonsbergen et al., 2005). D. Collapse of DSGSDs related to rock massifs weakened by prolonged karstification (e.g. Pánek et al., 2009b). E. Flexural toppling may drive genesis of the hinge zone delimited by slip surface at the maximum bending curvature of the strata. In such circumstances, rotational landslides eventually transforming to catastrophic rock slope failures may occur (e.g. Chigira and Kiho, 1994). F. Block toppling producing slope collapse by overturning of discontinuities (e.g. bedding or schistosity planes) to unstable position (e.g. Pánek et al., 2009a). G. Lateral spreading of competent rocks overlying ductile clayey formations may initiate recurrent earthflows due to the collapse of rigid rock slabs and resulting undrained load within plastic material (e.g. Bisci et al., 1996).

shape and particle size distribution that determine the evolution of the mechanical behavior of the material (Lebourg et al., 2011). Declines in rock strength also result from subcritical crack growth (Brückl and Parotidis, 2001) in environments without pre-existing discontinuity planes, repeated actions of groundwater pressure (Vallet et al., in press) or weathering whose role depends, among others, on fracture properties of rock mass and climate (Lebourg et al., 2011).

Although opinions whether chronic deep-seated movements of slopes inescapably lead to accelerated movements vary (Bovis and Evans, 1996; Hewitt et al., 2008; Chigira et al., 2013), an increasing number of case studies related to catastrophic rock slope failures from diverse mountain settings (especially Pacific Coast Ranges, Rocky Mountains, Andes, Norway, Scottish Highland, European Alps, Apennines, Carpathians, Himalayas, Japan, Taiwan and Southern Alps of New Zealand) provide an insight into this question. We describe separately (i) accelerated, highly localized and rather moderately moving (10^{-1}–10^{2} m year^{-1}) failures involving translational and rotational landslides; (ii) earthflows related to lateral spreading phenomena;

and (iii) large-scale rock avalanches and rockslides representing extremely fast and the most hazardous end-members of rock slope instabilities.

6.1. Progressively developing landslides within DSGSDs

Long-lasting accelerated deformations within localized zones of DSGSDs lead often to progressive development of morphologically distinct landslide bodies (Fig. 12). This development is frequently preceded by periods of accelerated movements within specific parts of DSGSDs, often exceeding the general deformation rate by order of magnitude (Le Roux et al., 2011). Although some studies reveal accelerated movements close to DSGSD depletion areas (Brückl and Parotidis, 2005; Barla et al., 2010; Strozzi et al., 2013), the most typical zone of landslide formation within DSGSDs is at the toe due to most intensive shear stresses at the base of rock slopes (Guglielmi and Cappa, 2010) and the presence of highly fractured (El Bedoui et al., 2009; Lebourg et al., 2011; Le Roux et al., 2011; Agliardi et al., 2012) or more plastic rocks (Berardino et al., 2003) and unconsolidated sediments (Newman, 2013). An instructive example is the La Clapière landslide in the SE French Alps. After ~10 ka of slow deformation rates (<30 mm year^{-1}), part of the sackung-affected slope with volume about 60×10^6 m^3 accelerated its movement to >80 mm year^{-1} with some periods exceeding 1 m year^{-1} (El Bedoui et al., 2009). As a result, a landslide has developed in the lower part of the DSGSD since the 1960s (Fig. 12). Similarly, increased movement activity of well-developed rockslide with surface velocities of up to 1.6 m day^{-1} within sackung was reported by Crosta et al. (2014).

On the regional scale, preferential clustering of rotational and translational landslides within zones affected by sackung-type DSGSDs or large-scale lateral spreading has been recognized for decades (e.g. Němčok, 1972; Dramis and Sorriso-Valvo, 1994; Agliardi et al., 2001, 2012; Baroň et al., 2004; Korup, 2005; Kellerer-Pirklbauer et al., 2010; Pánek et al., 2011a; Capitani et al., 2013 etc.). A close link between the spatial distribution of DSGSDs and shallower mass movements is suggested by some landslide susceptibility studies. Based on statistical modeling of the distribution of translational landslides within the mountains of Tuscany (Italy), Capitani et al. (2013) revealed that DSGSDs significantly affect landslide distribution, especially in areas with mechanically strong rocks. Similar conclusions come from the Argentera massif (French Alps), where landslides are ubiquitous in sedimentary rocks, but landslides in metamorphic rocks are found almost exclusively within DSGSD areas (Jomard et al., 2014). These findings support the assumption that DSGSDs may give rise to landslides in rock types that have otherwise low susceptibility to shallow mass movements. Sorriso-Valvo et al. (1999) also showed that for sackungen from the Calabrian Apennines (Italy), accelerated deformations within the DSGSDs (accompanied by physical degradation of the rock mass and mobilization of numerous small shallow landslides) might dramatically increase sediment flux and cause repeated fluvial aggradation on adjacent alluvial plains or fans (Fig. 13).

6.2. Earthflows related to large-scale lateral spreading

Long-runout, episodically reactivated earthflows are often associated with lateral spreading phenomena that occur where thick fractured slabs of rigid rocks overlie material with plastic behavior (Bisci et al., 1996; Rohn et al., 2004; Marschallinger et al., 2009; Unkel et al., 2013). Deep-seated spreading of competent beds may activate earthflows, mainly due to the collapse of rock blocks at the flanks of the spreading rock slopes, which causes undrained loading in the underlying ductile substratum, and water percolation through the system of opened fractures within rigid rocks, leading to saturation of the lower weak bedrock. The stress generated by the caprock is accommodated by laterally unconfined ductile flow within the underlying plastic rock. The resulting earthflows generally undergo time-limited (lasting several days to months), pulse-like evolution, in which individual reactivations may mobilize large amounts of material (>10^6 m^3) and horizontally move several hundred meters to a few kilometers. The recurrence interval of such mass movements is on the order of 10^{-1}–10^3 year (Bisci et al., 1996; Pánek et al., 2011b; 2013; Unkel et al., 2013).

A spectacular example of such a reactivated 5.4-km long earthflow occurred in the Marche Region of central Italy (Sant'Agata Feltria earthflow; Bisci et al., 1996). Historical records indicate that the earthflow has been reactivated at least 12 times since the 16th century, often with highly destructive consequences for local settlements. This earthflow is a surficial side-effect of large-scale lateral spreading involving the upper part of the slope composed of thick fractured sandstone slabs that move above underlying soft clays (Bisci et al., 1996). During extreme hydrometeorological events, large tension cracks within the sandstone complex allow deep water to percolate, saturating the underlying soft rocks. During individual events, earthflows reactivated >3×10^6 m^3 of material (Bisci et al., 1996). Even larger earthflows have been documented in the North Calcareous Alps of Austria (Fig. 14; Rohn et al., 2004; Marschallinger et al., 2009; Unkel et al., 2013). As for the Stambach earthflow, three major rockfalls of Jurassic limestone from a lateral spread on Mt. Rauschberg activated an earthflow of Triassic and Jurassic marls in 1982 with a volume of ~8×10^6 m^3 (Unkel et al., 2013). Buried tree stumps in the earthflow material indicate that this particular event was preceded by four Holocene events at ~8, 5.7, 1.9 and 1.3 ka BP (Unkel et al., 2013). Numerous cases of similar earthflows have been described also from the Western Carpathians. Based on ^{14}C dating, Pánek et al. (2013) estimated for the Flysch Carpathians (Czech Republic, Slovakia) typical recurrence intervals of ~1–2 ka for earthflows that originated on the central or lower parts of slopes due to the partial collapses of predominantly lateral spreading-

Fig. 12. La Clapière landslide originated since the 1960s due to acceleration of movements in the lower part of DSGSD affecting entire SW flank of the Mount Colle Longue (Argentera massif, French Alps). Red arrows show location of trenches related to slow moving large-scale slope deformation (photo courtesy: T. Lebourg).

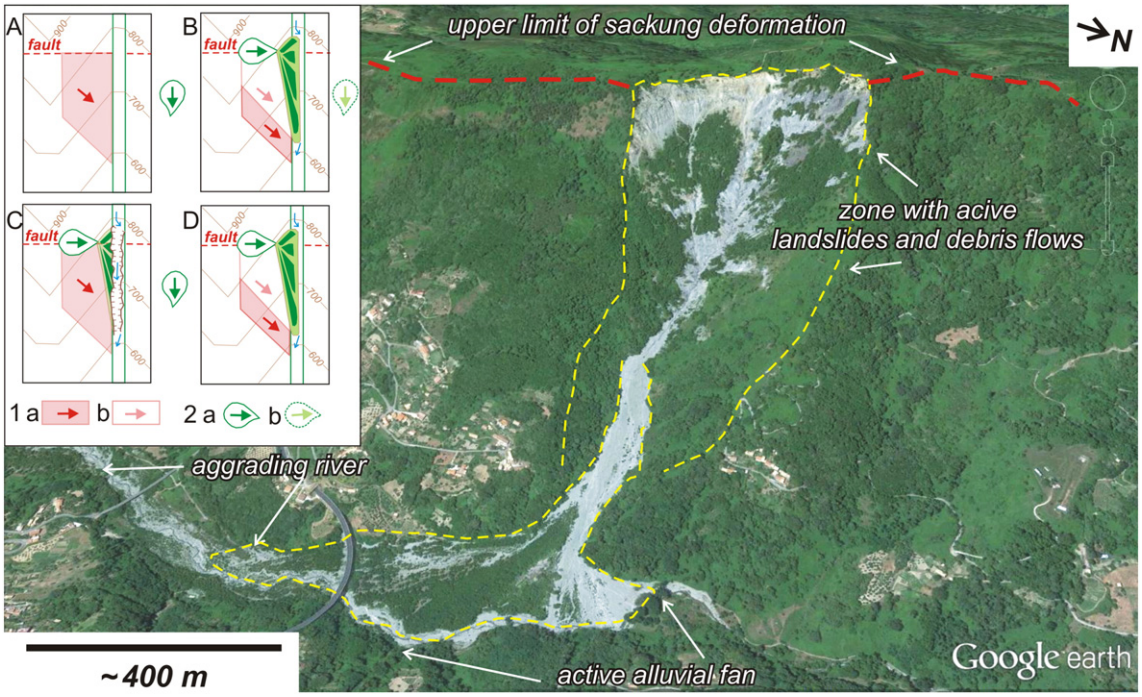

Fig. 13. Pizzotto-Greci slope (Calabria, Italy) as an example of the relationship between DSGSDs activity, production of shallow landslides/debris flows and the resulting aggradation pulses forming adjacent alluvial fan. Inserted scheme (adopted from Sorriso-Valvo et al., 1999) displays changing activity of DSGSDs in various time sequences (A–D) in relation to the buttressing effect of thick alluvia supporting the toe of the slope. Each phase of the river incision is associated with the sackung activation accompanied by shallow landslides and debris flow eventually leading to the building of adjacent alluvial fan and the river aggradation. Captions: 1a — active part of DSGSD, 1b — stabilized part of DSGSD, 2a — active stage of the debris flow source, 2b — inactive stage of the debris flow source. Google Earth image depicts main landform elements as presented in geomorphic map by Sorriso-Valvo et al. (1999).

related DSGSDs. The deformed southern slope of Mount Girová, eastern Czech Republic, produced at least two major (>2 × 10^6 m^3) and several secondary earthflows and shallow landslides during the last ~7.5 ka (Pánek et al., 2011b).

6.3. Rock avalanches from DSGSD collapses

Some of the largest recent rock avalanches occurred within DSGSDs (Boultbee et al., 2006; Hewitt et al., 2008; Chigira, 2009; Jaboyedoff

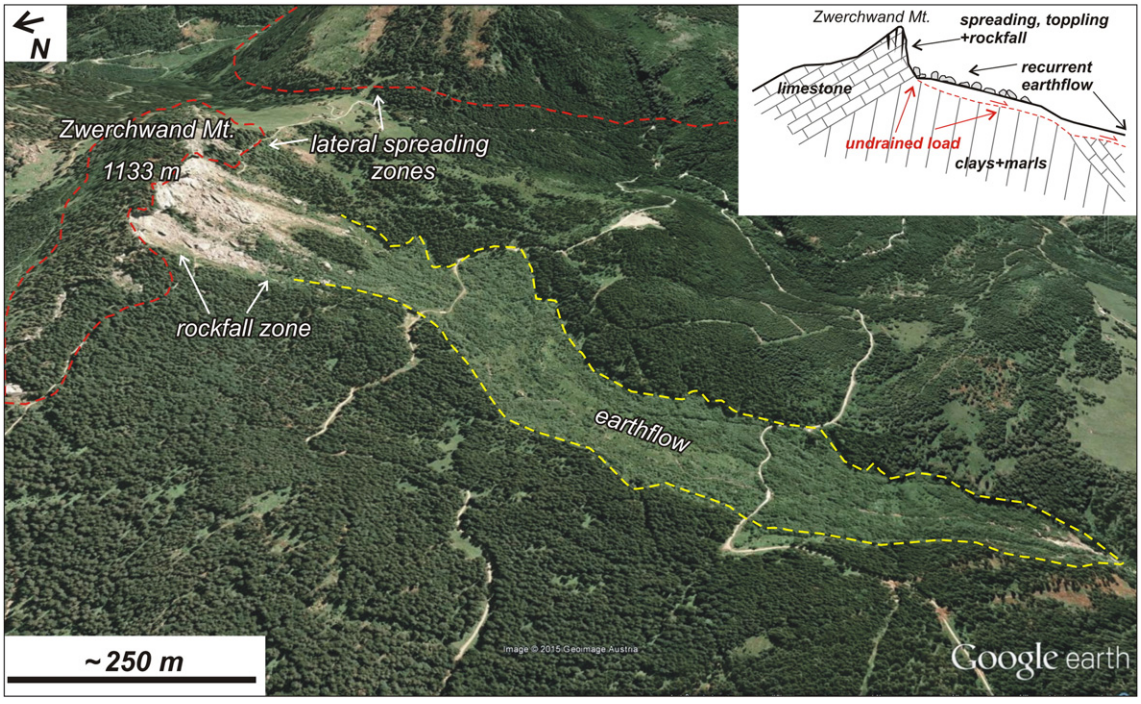

Fig. 14. Google Earth image of the Stambach earthflow (North Calcareous Alps, Austria) periodically reactivated by rockfalls from the laterally spread Zwerchwand Mt. Inserted cross-section adopted from Wilson et al. (2003) depicts schematically geology and mechanism of mass movements.

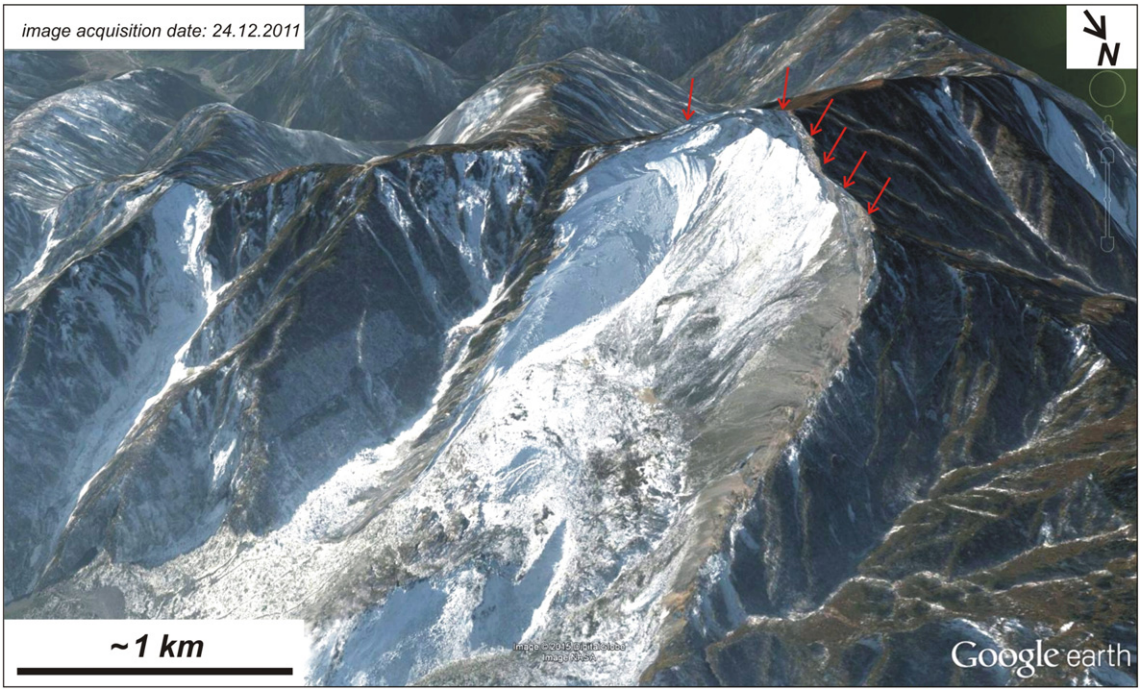

Fig. 15. Google Earth image of the Daguangbao rockslide (0.8 km^3) originated during the 2008 Wenchuan earthquake (Sichaun, China). It is among the largest recent catastrophic failures spatially associated with DSGSDs. Red arrows denote position of linear depression which is traceable on satellite images long before the slope collapse (Chigira et al., 2010).

et al., 2009; Chigira et al., 2010, 2013). One of the most pronounced examples of DSGSD related failures with volumes >10^8–10^9 m^3 occurred near the epicentral area of the 2008 Wenchuan earthquake (Chigira et al. 2010). Remote sensing data for the ridge affected by the ~0.8 km^3 Daguangbao rockslide reveal that the slope failure was preceded by 2-km-long ridge-top linear depression and pronounced bulging features revealing large scale gravitational spreading (Fig. 15; Chigira et al., 2010). Other major rockslides such as the Tangjiashan failure that formed the largest landslide dam in the area (Chigira et al., 2010) affected slopes that were gravitationally deformed long before the earthquake. A notable cluster of large-scale rockslides (~10^6–10^7 m^3) nested within DSGSDs was generated by September 2011 Typhoon Talas in the Kii peninsula (Honshu, Japan). Chigira et al. (2013) demonstrate that despite the fact that all of these rockslides originated on slopes with

Table 5
Examples of catastrophic rockslides and rock avalanches related to DSGSDs.

Location	Timing	Volume of collapse (10^6m^3)	Trigger	Comment	References
Hope slide/British Columbia (Canada)	9. 1. 1965	47	Not specified	Result of a very long-term mountain slope deformation preceded at least by one slope failure	Brideau et al. (2005)
Zymoetz River/British Columbia (Canada)	8. 6. 2002	1	Not specified	Result of a progressive degradation of altered rock mass on glacially over-steepened cirque walls preceded by at least one slope failure	Boultbee et al. (2006); McDougall et al. (2006)
Todagin Creek/British Columbia (Canada)	3. 10. 2006	4	Not specified, likely strong diurnal temperature changes	At least one major prehistoric rockslide (~8.4 ka BP) preceded modern failure	Sakals et al. (2012)
Sierre/Swiss Alps	>9.6 ka BP	1500	Not specified, likely seismicity or progressive degradation of the rock mass following deglaciation	Sackung features and buckling folding on the dip slope preceded origin of the failure	Pedrazzini et al. (2013)
Val Pola/Italian Alps	28. 7. 1987	34–43	Heavy rainfalls and extremely warm weather	Within slope section deformed by DSGSD and prehistoric landslide	Crosta et al. (2004)
Vaiont/Italian Alps	9. 10. 1963	270–300	Anthropogenic controlled water-level fluctuations on reservoir	Reactivation of large post-glacial rockslide, giant wave that overflowed the dam destroyed the village of Longarone and killed over 2000 people	Paronuzzi and Bola (2012)
Campo di Giove/Central Apennines (Italy)	Post 0.75 Myr	5.7	Not specified, likely seismicity	Several others Late Quaternary rock avalanches related to DSGSDs were described form the Central Apennines (see Bianchi Fasani et al. (2014))	Di Luzio et al. (2004); Bianchi Fasani et al. (2014)
Daguangbao/Longmen Shan range (China)	12. 5. 2008	837	M_w 7.9 Wenchuan earthquake	DSGSD with 2 km long linear depression near the top of mountain preceded rock avalanche, many other rock avalanches originated during the Wenchuan earthquake initiated on slopes affected by DSGSDs	Chigira et al. (2010)
Nonoo/Kyushu (Japan)	6. 9. 2005	3.3	Heavy rainfalls (two-days precipitations >1000 mm) connected with Typhoon 0514	Several other DSGSDs-related rockslides originated during 2005 Typhoon 0514 or later during the 2013 Typhoon Talas (Chigira et al., 2013)	Chigira (2009)
Cascade River/Southern Alps (New Zealand)	~1.4 ka BP	750	Likely high-magnitude ca 660 AD earthquake on the Alpine Fault	Source area of the rock avalanche is situated in the large scale asymmetric sackung.	Barth (2014)

DSGSDs, major failures only affected sites exposed to additional loading; in this case slope sections undercut by rivers. DSGSDs without direct contact to rivers remained stable (Chigira et al., 2013).

Many documented prehistoric rock avalanches and rockslides originated on slopes undergoing deep-seated gravitational spreading (Table 5), for example in the Scottish Highlands (Jarman, 2006; Ballantyne et al., 2014), Norway (Blikra et al., 2006; Böhme et al., 2013), European Alps (Pedrazzini et al., 2013), Carpathians (Pánek et al., 2009a), Karakoram Himalaya (Hewitt, 2006) and Southern Alps of New Zealand (Barth, 2014). In the Apennines, gravitational spreading of mountain ridges is among the most important factors driving occurrence of large-scale rock avalanches (Di Luzio et al., 2004; Esposito et al., 2013; Bianchi Fasani et al., 2014). For example, the Campo di Giove rock avalanche that mobilized >0.2 km^3 of material had its source area within the double-crested ridge intersected by numerous linear trenches (Di Luzio et al., 2004; Table 5).

Slowly moving DSGSDs provide preconditioning or preparatory factors (sensu Glade and Crozier, 2005) for catastrophic rock slope failures.

Table 6
Preconditions and causes of twenty world most important recent catastrophic rockslides and rock avalanches spatially associated with DSGSDs. 1) Existence of major preceding failure(s); 2) Presence of first-order pervasive discontinuities; 3) Rapidly uplifting landscape (usually >1 mm $year^{-1}$); 4) Slope undercut by river or intensive stream erosion within DSGSD; 5) Substantial deglaciation since the Little Ice Age; 6) Existence of mountain permafrost; 7) Without obvious trigger; 8) Earthquake preceding collapse; 9) Elevated pore pressures due to heavy rainfall, snowmelt or other factors; 10) Temperature anomaly before collapse.

Catastrophic collapse with the year of event/reference	Conditions									
	1	2	3	4	5	6	7	8	9	10
1. Hope Slide 1965/Brideau et al. (2005)	■	■	■	■			■			
2. Zymoetz River 2002/Boultbee et al. (2006)	■	■	■				■			
3. Pink Mountain 2002/Geertsema et al. (2006)	■	■				■			■	■
4. Todagin Creek 2006/Sakals et al. (2012)	■	■	■	■		■	■			
5. Mosque Mountain mid 1990s/Lu et al. (2003)	■	■	■			■	■			
6. East Gate 1997/Brideau et al. (2006)	■	■	■			■	■			
7. Devastation Creek 1975/Holm et al. (2004)	■	■	■		■	■	■			
8. Frank Slide 1903/Cruden and Martin (2007)	■	■		■			■			
9. Tafjord 1934/Blikra et al. (2006)	■	■	■				■			
10. Vaiont 1963/Paronuzzi and Bola (2012)	■	■		■					■	
11. Val Pola 1987/Crosta et al. (2004)	■	■	■	■		■			■	■
12. Yigong 2000/Zhou et al. (2015)	■	■	■		■	■			■	■
13. Guanling 2010/Yin et al. (2011)	■	■							■	
14. Daguangbao 2008/Chigira et al. (2010)		■	■	■				■		
15. Aresawa 2004/Nishii et al. (2013)	■	■	■			■			■	
16. Nonoo 2005/Chigira (2009)		■	■	■					■	
17. Akatani 2011/Chigira et al. (2013)	■	■	■	■					■	
18. Tsaoling 1999/Chigira et al. (2003)	■	■	■	■				■		
19. Chiu-fen-erh-shan 1999/Wang et al. (2003)		■	■	■				■		
20. Young River 2007/Massey et al. (2013)		■	■	■			■			

References cited in Table 6: Brideau et al. (2005); Boultbee et al. (2006); Geertsema et al. (2006); Sakals et al. (2012); Lu et al. (2003); Brideau et al. (2006); Holm et al. (2004); Cruden and Martin (2007); Blikra et al. (2006); Paronuzzi and Bola (2012); Crosta et al. (2004); Zhou et al. (2015); Yin et al. (2011); Chigira et al. (2010); Nishii et al. (2013); Chigira (2009); Chigira et al. (2013); Chigira et al. (2003); Wang et al. (2003); and Massey et al. (2013).

The eventual triggers include seismic loading, heavy rainfall or rapid snowmelt (Chigira et al., 2010, 2013). An analysis of conditions leading to some of the most significant recent catastrophic collapses associated with DSGSDs reveal that, besides the existence of previous instabilities, distinct bedrock discontinuities, and seismic activity, the immediate causes vary from case to case (Table 6). Nine of the recent DSGSDs-related catastrophic collapses did not have any obvious trigger. In such circumstances progressive weakening of the bedrock, i.e. the preparation of sufficient volume of the rock mass with reduced strength, during DSGSD motion might play crucial role for rock-slope failure. The remaining catastrophic failures were triggered by seismic loading, heavy rainfall or rapid snowmelt, especially where slopes were undercut by rivers (Table 6; Chigira et al., 2010, 2013). Deglaciation since the Little Ice Age possibly affected only two of the examined catastrophic collapses. Rocks exposed in source areas of rock avalanches are often pervasively fragmented, promoting failures from the same slope sections. Böhme et al. (2013) showed that DSGSD slopes in metamorphic rocks at Stampa (Norway) produced at least three rock avalanches during the Holocene.

7. Concluding remarks

7.1. Recent progress in the understanding of temporal behavior of DSGSDs

When summarizing the growing body of literature on the long- and short-term DSGSDs dynamics, the main findings that emerged especially since the turn of 21st century are as follows:

i) DSGSDs may be active on 10^4 year time scales, but their lifespan is seemingly biased to younger periods due to the limited time-range of available dating methods;
ii) More complex and generally longer lifespans reveal DSGSDs located outside the limits of Quaternary glaciations;
iii) The style of movements (creep versus episodic) may be related to rock brittleness, but this relationship should be verified by a substantially larger body of further study;
iv) Episodic movements are very often related to seismic activity, especially when DSGSDs are superimposed onto tectonically active structures;
v) Short-term temporal displacements derived from high-resolution monitoring resemble movement patterns obtained for ~10^3–10^4 year time series;
vi) Catastrophic rock slope failures, such as rock avalanches nested within DSGSDs, often collapse without any obvious trigger.

The long- and short-term dynamics of DSGSDs revealed by their dating and monitoring are continuous and partly cyclic processes, where the outcomes of short-term development (e.g. episodic reactivations) affect the settings that control their long-term behavior (e.g. creep; Fig. 16). At the same time, these settings controlling long-term behavior (e.g. creep) provide the preconditions for the possible occurrence of short-term activity, which is also strongly accentuated by independent variables represented by the triggers of accelerated deformations (Fig. 16). The complexity of this behavior and its underlying physical processes has been described by advanced numerical models applied to the DSL (Preisig et al., 2016). This work presents a conceptual framework linking hydromechanical cycling, progressive failure and rock fatigue in order to explain creep as well as episodic accelerations lacking obvious triggers. Despite the fact that the limited number of dated DSGSDs (Table 3) prevents detailed evaluation of the factors contributing to their chronological behavior, it seems that the lifespan of DSGSDs is influenced especially by rock mass properties (lithology and structure), tectonic conditions, recent and past climatic settings and deglaciation history of a given region. Dating results show more complex and often significantly longer life spans of DSGSDs and DSLs found in non-glaciated settings. This fact could be attributed to the erasing of evidence of DSGSDs during enhanced glacier activity in the Last Glacial Maximum and more generally to the high erosion rates characterized for glaciated mountain ranges (Herman et al., 2013). Recent studies show that sequestration of mass movement products by glaciers could be very rapid, ranging from days to a few months for rock avalanches exceeding a volume of 10^6 m^3 (Dunning et al., 2015). Therefore, catastrophically failed DSGSDs as well as fragmented rocks from disrupted slopes were likely to have been effectively evacuated from mountain valleys during the Last Glacial Maximum. Apart from the absence of major erosion agents such as glaciers, non-glaciated mountains usually reveal reduced local relief, and are often situated in more continental, semi-arid or arid settings (Korup et al., 2007). All of these factors contribute to the lower erosion rates in these areas and thus provide the potential for the longer existence of the morphology of DSGSDs, and their sedimentary evidence and/or non-disturbed evolution. However, regardless of whether they are situated in formerly glaciated or non-glaciated mountains, DSGSDs in some extremely weak rocks, such as

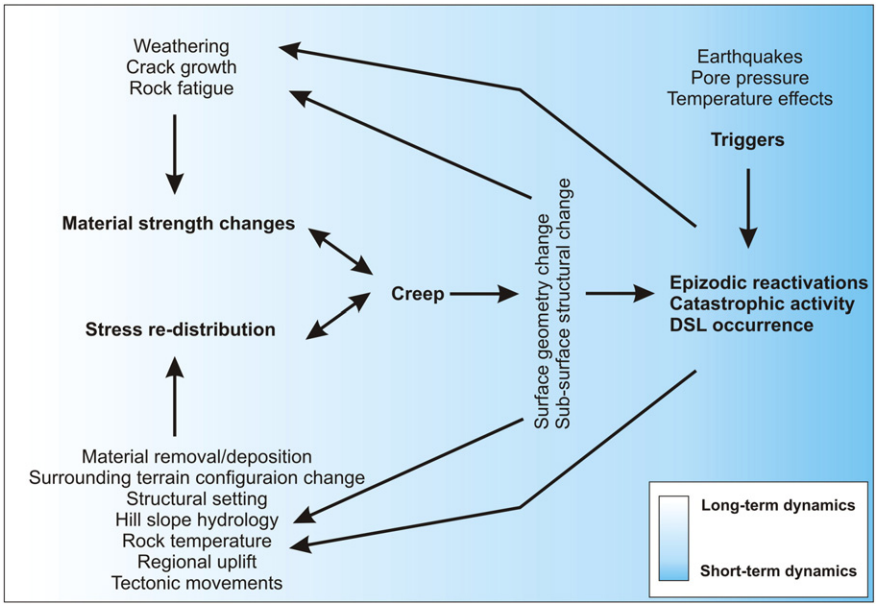

Fig. 16. Chart showing the main relationships between different processes and the conditions affecting the long- and short-term dynamics of DSGSDs.

flych, reveal short lifespans rarely exceeding the time span of the Holocene (Margielewski, 2006; Pánek et al., 2011a; Urban et al., 2013). It is also worth noting that geochronologically-inferred deformation rates and lifespans differ between DSGSDs and DSLs. Although the dataset of chronologically constrained features with reconstructed movements is still limited (Table 3), DSLs usually reveal much higher long-term deformation rates (~10^2 mm year^1) and shorter lifespans (often <10^4 years) than DSGSDs (Fig. 4). Therefore, the results of dating could shed more light on the differences between both phenomena, as the use of geomorphological and structural criteria only could be misleading.

Another avenue of progress lies in the understanding of the types of movements and rates of DSGSD displacements. Before the first monitoring and dating studies, creep was considered as a dominant mode of DSGSD movements (Varnes et al., 1990). Although it should still be considered as an important regime of DSGSD movements (some studies confirm creep as prevailing mode for the majority of lifespan of some dated DSGSDs; McCalpin and Irvine, 1995; McCalpin et al., 2011 etc.), available data show that both short- and long-term deformations of some DSGSDs are dominated by episodic movements, especially where superimposed on active tectonic structures (McCalpin and Hart, 2003; Gutiérrez et al., 2008; Moro et al., 2012). However, similarly as in connection with the lifespans, the types and rates of DSGSD movements are seemingly influenced by mechanical properties of rocks involved in gravitational deformation. Although Hippolyte et al. (2012) suggested a link between the type of DSGSDs movements (e.g. creep versus episodic movements) and the brittleness of rocks, this assumption should be further tested by dating, monitoring and modeling a substantially larger sample of slope deformations affecting contrasting rock types.

One of the key open questions regards the transformation of slow DSGSD movements to catastrophic collapses. The main message from numerous case studies is that the majority of inventoried DSGSDs experienced no large-scale collapses (Hewitt et al., 2008; Agliardi et al., 2012; Crosta et al., 2014), although many DSGSDs contain sectors with frequent occurrences of small scale, fast moving rockfalls or slides (Brückl and Parotidis, 2005; Barla et al., 2010; Le Roux et al., 2011; Crosta et al., 2014). On the other hand, many rock-slope failures involving the largest rock avalanches (>10^8–10^9 m^3, Chigira et al., 2010; Barth, 2014; Bianchi Fasani et al., 2014 etc.) are spatially linked to features diagnostic of DSGSDs such as trenches, antislope scarps, tension cracks and buckling (Jomard et al., 2014), indicating that collapses were preceded by phases of slope sagging. This may lead to progressive weakening of the bedrock which alone may be sufficient for the production of catastrophic failures, as evidenced by DSGSD-related catastrophic collapses without obvious triggers (Table 6). This is supported by mechanical models revealing that time-dependent progressive damage of intact rock, concentration of deformation on sliding surface and its progressive smoothing might have lasted for several thousands of years with final transition to rapid sliding (Brückl and Parotidis, 2005; Lacroix and Amitrano, 2013). These models show that catastrophic collapses occur when several time-dependent variables (e.g. progressively changed strength of involved material, occurrence of triggering events) and spatial variables (e.g. lithological properties and structure) coincide.

7.2. Remaining research challenges

The main future research challenges and the recommended focus of research are summarized in Table 7. Despite the new findings, it should be stressed that a lot of the new information about the temporal behavior of DSGSDs is based on only a limited number of case studies and there are still many open unsolved or only partly solved questions. In summary, the main deficit in the knowledge of the temporal dynamics of DSGSDs can be attributed to three main deficiencies involving (i) the limited database of dated and monitored DSGSDs, (ii) insufficient resolution and missing coupling between data related to long- and

Table 7
Summary of major future research goals for the investigation of the temporal behavior of DSGSDs.

Wider research topics	Main specific questions	Suggested approach[a]
Lifespan and long-term (≥10^2 year) evolution of DSGSDs	• What is the maximum lifespan of DSGSDs? • How do lithological, tectonic and climatic factors influence the lifespan of DSGSDs? • Could certain DSGSDs provide palaeoenvironmental (esp. palaeoclimatic) signals? • To what degree do past DSGSDs reflect the timing of palaeoearthquakes? • Could the development of certain DSGSDs reflect the influence of odd/rarely discussed triggers (e.g. sea-level changes, permafrost degradation)?	• *Regional-scale DSGSD dating and correlation with high-resolution palaeoenvironmental/paleoseismological proxies* • Extension of databases of dated DSGSDs into various types of morphoclimatic regions • Application of new dating methods and strategies • *Testing of high-resolution dating methods spanning the last few centuries* (e.g. *dendrochronology*), i.e. *time period for which radiometric dating is too imprecise and monitoring data are not available*
Style of DSGSD movements	• Which prevail: creep, episodic movements or a combination of both mechanisms? • Could episodic or accelerated movements of DSGSDs be related to high magnitude triggers such as strong earthquakes or heavy rainfalls? • Do predictable spatio-temporal trends in the evolution of DSGSDs exist? • Catastrophic failure of DSGSDs: rule or singularity? • How significantly do the DSGSDs material properties change over their lifespan?	• *Combination of widespread dating and monitoring on the same DSGSDs* • Dating and comparison of the timing of DSGSDs with the ages of adjacent products of catastrophic rock slope failures • Improvements of InSAR and other remote sensing techniques for capturing information about spatial deformation patterns • *Inclusion of time in 2D and 3D numerical models of DSGSDs* • *Strength testing and petrographic analysis of dated materials of DSGSDs*
Role of glacial cycles in DSGSD development	• How many (if any) glaciations may DSGSDs survive? • Can DSGSDs originate during periods of full glaciation? • What is the response time of the onset of DSGSDs after glacier withdrawal?	• Focus on DSGSDs dating in areas with an established high-resolution history of deglaciation • Focus on mapping and monitoring of DSGSDs on recently deglaciated terrains • Quantification of the rate of glacial sequestration of mass movement deposits • Numerical modeling of slope response to deglaciation
Short-term DSGSD (<10^2 year) activity	• What are the main triggers of the first-time occurrence of DSGSDs? • How do predisposing factors of the first-time occurrence of DSGSDs differ from the actual conditions? • Which external and internal variables control short-term fluctuations of DSGSD activity? • Is the catastrophic failure of DSGSDs predictable from measured deformation trends alone?	• *Combination of 2D and 3D precise ground and underground monitoring techniques and their combination with remote sensing methods* (*InSAR*, *scanning from unmanned aerial vehicles* etc.) *for capturing spatial trends of surface and sub-surface movements on DSGSDs movements* • Numerical modeling of the response of DSGSDs to various types of triggers • Reconstruction of topographic, hydrogeologic and lithologic conditions preceding the first-time occurrence of DSGSDs • *Monitoring of deep aquifers* (e.g. *geochemistry*), *continual geophysical* (e.g. *resistivity*) *measurements*

[a] (Suggestions in italic represent rarely applied approaches).

short-term evolution of individual DSGSDs and finally (iii) poor data on the deep internal structure, material properties and their temporal changes on slopes affected by DSGSDs.

It seems that many of the uncertainties about the lifespan of DSGSDs result from the simple fact that most of the dating and monitoring performed to date has been focused on similar types of settings. Our knowledge about the temporal dynamics of DSGSDs is thus biased, especially concerning alpine mountains in temperate zones. We suggest geographically expanding DSGSD investigations to regions that are known to have large-scale mass movements (e.g. Korup et al., 2007) but lack any chronological or monitoring data about DSGSDs. This is the case for the Andes, Himalayas or mountains of Central Asia, as well as settings where the occurrence of DSGSDs is confirmed but recent climatic conditions are unfavorable for the emergence and activity of DSGSDs (e.g. hyperarid regions of the Atacama or Sahara; Busche, 2001; Pinto et al., 2008). This will result in an extension of the database of dated and monitored cases of contrasting landscapes, which will provide deeper knowledge about the role of lithology, tectonics and climate in the temporal evolution of DSGSDs.

Other deficiencies clearly result from the insufficient spatial resolution of dating and monitoring as well as a lack of DSGSDs where dating and monitoring have been effectively combined (Hermanns et al., 2013). Without such an approach it will be difficult to recognize more effectively the styles of DSGSD movements and their triggers. Therefore, it is necessary to perform more studies where the long-term displacement rates inferred from chronological studies are coupled with recent high-resolution monitoring. Furthermore, we suggest focusing on the acquisition of high-resolution data revealing spatio-temporal displacement trends across entire DSGSD bodies in order to understand the localization of accelerated movements and to predict possible catastrophic collapses of DSGSDs. Regarding short-term displacements, we assume that the most important new information on DSGSD movement detection will encompass surface and sub-surface data from wireless instruments allowing 3D measurements and their reliable combination with remote sensing techniques involving high-resolution satellite data (e.g. TerraSAR-X, Radarsat-2, Sentinel-1; Strozzi et al., 2013) and their low-cost alternatives such as scanning from unmanned aerial vehicles (UAV) and fast and accurate optical image processing algorithms (e.g. structure for motion, Remondino et al., 2011; Turner et al., 2015).

A promising step taken in recent years has been the inclusion of absolute time-scales to both numerical models of individual slope deformations (Eberhardt et al., 2007; Lacroix and Amitrano, 2013; Preisig et al., 2016) and to regional-scale geomechanical models of progressive rock slope failures (Guglielmi and Cappa, 2010). However, models have so far only been applied on kinematically simpler DSLs and usually contain hypotheses which are difficult to validate or are based on simplified mathematical solutions of complex physical processes (e.g. Vallet et al., in press; Brückl and Parotidis, 2005). Some of the simplifications (e.g. assumption of constant hydrogeological conditions, Preisig et al., 2016) are acceptable for time intervals of 10^1 years but may represent an oversimplification if the behavior of DSGSDs at a time scale of 10^3–10^4 years needs to be explained. Application of advanced numerical models in DSGSD chronological studies is therefore limited due to their extreme length of development and the complexity of the settings. Other factors affecting the application of these models include their large size, a lack of data on the rock mechanical properties and their change over extended time periods, and poor information regarding the deep structure and hydrogeology of mountain slopes. Therefore, the future successful extension of advanced numerical modeling of DSGSDs is dependent on focused and improved geotechnical processing (e.g. time dependent change of mechanical properties of DSGSD material), geophysical research of the whole mountain slope and the correct description of deep aquifer water circulation. With such updated parameters, numerical models would significantly contribute to the understanding of crucial chronological characteristics, such as the time span needed for DSGSDs to transform from their incipient stage to possible catastrophic collapse or their time response to various triggers, such as the commonly discussed glacier withdrawal.

Acknowledgments

This study was conducted within the framework of the Czech Science Foundation, project 13-15123S. Special thanks are extended to Dr. Giovanni Bertolini, Prof. Francesco Dramis, Dr. Thomas Lebourg and Dr. Marino Sorriso-Valvo for providing field photos. We express our sincere gratitude to Oliver Korup for discussion on the topic of this work and help with manuscript polishing, to Isaac Larsen and an anonymous reviewer for their valuable comments that substantially improved the manuscript. This work was carried out also thanks to the support of the long-term conceptual development research organization RVO: 67985891.

References

Agliardi, F., Crosta, G.B., Zanchi, A., 2001. Structural constrains on deep-seated slope deformations kinematics. Eng. Geol. 59, 83–102.
Agliardi, F., Crosta, G.B., Zanchi, A., Ravazzi, C., 2009a. Onset and timing of deep-seated gravitational slope deformations in the Eastern Alps, Italy. Geomorphology 103, 113–129.
Agliardi, F., Zanchi, A., Crosta, G.B., 2009b. Tectonic vs. gravitational morphostructures in the Central Eastern Alps (Italy): constraints on the recent evolution of the mountain range. Tectonophysics 474, 250–270.
Agliardi, F., Crosta, G.B., Frattini, P., 2012. Slow rock-slope deformation. In: Clague, J.J., Stead, D. (Eds.), Landslides Types. Cambridge University Press, Mechanisms and Modeling, pp. 207–221.
Agliardi, F., Crosta, G.B., Frattini, P., Malusà, M., 2013. Giant non-catastrophic landslides and the long-term exhumation of the European Alps. Earth Planet. Sci. Lett. 365, 263–274.
Alexandrowicz, Z., Alexandrowicz, S.W., 1988. Ridge top trenches and rifts in the Polish Outer Carpathians. Ann. Soc. Geol. Pol. 58, 207–228.
Alexandrowicz, Z., Margielewski, W., 2010. Impact of mass movements on geo- and biodiversity in the Polish Outer (Flysch) Carpathians. Geomorphology 123, 290–304.
Ambrosi, C., Crosta, G.B., 2006. Large sackung along major tectonic features in the Central Italian Alps. Eng. Geol. 83, 183–200.
Apuani, T., Corazzato, C., 2009. Numerical model of the Stromboli volcano (Italy) including the effect of magma pressure in the dyke system. Rock Mech. Rock. Eng. 42, 53–72.
Bachmann, D., Bouissou, S., Chemenda, A., 2009. Analysis of massif fracturing during deep-seated gravitational slope deformation by physical and numerical modeling. Geomorphology 103, 130–135.
Ballantyne, C.K., Sandeman, G.F., Stone, J.O., Wilson, P., 2014. Rock-slope failure following Late Pleistocene deglaciation on tectonically stable mountainous terrain. Quat. Sci. Rev. 86, 144–157.
Barla, G., Antolini, F., Barla, M., Mensi, E., Piovano, G., 2010. Monitoring of the Beauregard landslide (Aosta Valley, Italy) using advanced and conventional techniques. Eng. Geol. 116, 218–235.
Baroň, I., Cílek, V., Krejčí, O., Melichar, R., Hubatka, F., 2004. Structure and dynamics of deep-seated slope failures in the Magura Flysch Nappe, Outer Western Carpathians (Czech Republic). Nat. Hazards Earth Syst. Sci. 4, 549–562.
Baroň, I., Kernstocková, M., Faridi, M., Bubík, M., Milovský, R., Melichar, R., Sabouri, J., Babůrek, J., 2013. Paleostress analysis of a gigantic gravitational mass movement in active tectonic setting: the Qoshadagh slope failure, Ahar, NW Iran. Tectonophysics 605, 70–87.
Barth, N.C., 2014. The Cascade rock avalanche: implications of a very large Alpine fault-triggered failure, New Zealand. Landslides 11, 327–341.
Beck, A.C., 1968. Gravity faulting as a mechanism of topographic adjustment. N. Z. J. Geol. Geophys. 11, 191–199.
Beget, J.E., 1985. Tephrochronology of antislope scarps on an alpine ridge near Glacier Peak, Washington, U.S.A. Arct. Alp. Res. 17, 143–152.
Berardino, P., Costantinib, M., Franceschettic, G., Iodicec, A., Pietranerab, L., Rizzod, V., 2003. Use of differential SAR interferometry in monitoring and modelling large slope instability at Maratea (Basilicata, Italy). Eng. Geol. 68, 31–51.
Bianchi Fasani, G., Di Luzio, E., Esposito, C., Evans, S.G., Scarascia Mugnozza, G., 2014. Quaternary, catastrophic rock avalanches in the Central Apennines (Italy): relationships with inherited tectonic features, gravity-driven deformations and the geodynamic frame. Geomorphology 211, 22–42.
Bigot-Cormier, F., Braucher, R., Bourlès, D., Guglielmi, Y., Dubar, M., Stéphan, J.F., 2005. Chronological constraints on processes leading to large active landslides. Earth Planet. Sci. Lett. 235, 141–150.
Bisci, C., Burattini, F., Dramis, F., Leoperdi, S., Pontoni, F., Pontoni, F., 1996. The Sant'Agata Feltria landslide (Marche Region, Central Italy): a case of recurrent earthflow evolving from a deep-seated gravitational slope deformation. Geomorphology 15, 351–361.
Blair, R.W., 1994. Mountain and valley wall collapse due to rapid deglaciation in Mount Cook National Park, New Zealand. Mt. Res. Dev. 14, 347–358.
Blikra, L.H., Longva, O., Braathen, A., Dehls, J.F., Stalsberg, K., 2006. Rock slope failures in Norwegian Fjord areas: examples, spatial distribution and temporal pattern. In:

Evans, S.G., Mugnozza, G.S., Strom, A., Hermanns, R.L. (Eds.), Landslides From Massive Rock Slope Failure. Springer, Dordrecht, pp. 475–496.
Bonci, L., Calcaterra, S., Cesi, C., Gambino, P., Gullí, G., Niceforo, C., Merli, K., Sorriso, M., 2010. Displacements on a slope affected by deep-seated gravitational slope deformation: Greci slope (Lago, Calabria, Italy). Geografia Fisica e Dinammica Quaternaria 33, 141–153.
Böhme, M., Hermanns, R.L., Oppikofer, T., Fischer, L., Bunkholt, H.S.S., Eiken, T., Pedrazzini, A., Derron, M.H., Jaboyedoff, M., Blikra, L.H., Nilsen, B., 2013. Analyzing complex rock slope deformation at Stampa, Western Norway, by integrating geomorphology, kinematics and numerical modeling. Eng. Geol. 154, 116–130.
Booth, A.M., Dehls, J., Eiken, T., Fischer, L., Hermanns, R.L., Oppikofer, T., 2014. Integrating diverse geologic and geodetic observations to determine failure mechanisms and deformation rates across a large bedrock landslide complex: the Osmundneset landslide, Sognog Fjordane, Norway. Landslides http://dx.doi.org/10.1007/s10346-014-0504-y.
Boultbee, N., Stead, D., Schwab, J., Geertsema, M., 2006. The Zymoetz River rock avalanche, June 2002, British Columbia, Canada. Eng. Geol. 83, 76–93.
Bovis, M.J., 1982. Uphill-facing (antislope) scarps in the Coast Mountains, Southwest British Columbia. Geol. Soc. Am. Bull. 93, 804–812.
Bovis, M.J., Evans, S.G., 1996. Extensive deformations of rock slopes in southern Coast Mountains, Southwest British Columbia, Canada. Eng. Geol. 44, 163–182.
Brideau, M.A., Stead, D., Kinakin, D., Fecova, K., 2005. Influence of tectonic structures on the Hope Slide, British Columbia, Canada. Eng. Geol. 80, 242–259.
Brideau, M.A., Stead, D., Couture, R., 2006. Structural and engineering geology of the East Gate landslide, Purcell Mountains, British Columbia, Canada. Eng. Geol. 84, 183–206.
Briestenský, M., Košťák, B., Stember, J., Vozár, J., 2011. Long-term slope deformation monitoring in the high mountains of the Western Carpathians. Acta Geodyn. Geomater. 164, 403–412.
Brückl, E., Parotidis, M., 2001. Estimation of large-scale mechanical properties of a large landslide on the basis of seismic results. Int. J. Rock Mech. Min. Sci. 38, 877–883.
Brückl, E., Parotidis, M., 2005. Prediction of slope instabilities due to deep-seated gravitational creep. Nat. Hazards Earth Syst. Sci. 5, 155–172.
Busche, D., 2001. Early quaternary landslides of the Sahara and their significance for geomorphic and climatic history. J. Arid Environ. 49, 429–448.
Capitani, M., Ribolini, A., Federici, R.R., 2013. Influence of deep-seated gravitational slope deformations on landslide distributions: a statistical approach. Geomorphology 201, 127–134.
Carbonel, D., Gutiérrez, F., Linares, R., Roqué, C., Zarroca, M., McCalpin, J., Guerrero, J., Rodríguez, V., 2013. Differentiating between gravitational and tectonic faults by means of geomorphological mapping, trenching and geophysical surveys. The case of the Zenzano fault (Iberian chain, N Spain). Geomorphology 189, 93–108.
Carton, A., Dramis, F., Sorriso–Valvo, M., 1987. Earthquake landforms: observations after recent Italian and Algerian seismic events. Zeitschrift für Geomorphologie. N. F., Suppl. Bd. 63, 149–158.
Coquin, J., Mercier, D., Bourgeois, O., Cossart, E., Decaulne, A., 2015. Gravitational spreading of mountain ridges coeval with Late Weichselian deglaciation: impact on glacial landscapes in Tröllaskagi, Northern Iceland. Quat. Sci. Rev. 107, 197–213.
Colesanti, C., Wasowski, J., 2006. Investigating landslides with space-borne synthetic aperture radar (SAR) interferometry. Eng. Geol. 88, 173–199.
Crosta, G.B., Agliardi, F., 2002. How to obtain alert velocity thresholds for large rockslides. Phys. Chem. Earth 27, 1557–1565.
Crosta, G.B., Chen, H., Lee, C.F., 2004. Replay of the 1987 Val Pola landslide, Italian Alps. Geomorphology 60, 127–146.
Crosta, G., Frattini, P., Agliardi, F., 2013. Deep seated gravitational slope deformations in the European Alps. Tectonophysics 605, 13–33.
Crosta, G.B., di Prisco, C., Frattini, P., Frigerio, G., Castellanza, R., Agliardi, F., 2014. Chasing a complete understanding of the triggering mechanisms of a large rapidly evolving rockslide. Landslides 11, 747–764.
Cruden, D.M., Varnes, D.J., 1996. Landslide types and processes. In: K., Turner A., L., Schuster R. (Eds.), Landslides Investigation and Mitigation. Transportation Research Board, US National Research Council. Special Report 247, Washington, DC, Chapter. Vol. 3, pp. 36–75.
Cruden, D.M., Martin, C.D., 2007. Before the Frank Slide. Can. Geotech. J. 44, 765–780.
Chigira, M., Kiho, K., 1994. Deep-seated rockslide-avalanches preceded by mass rock creep of sedimentary-rocks in the Akaishi Mountains, Central Japan. Eng. Geol. 38, 221–230.
Chigira, M., Wang, W.N., Furuya, T., Kamai, T., 2003. Geological causes and geomorphological precursors of the Tsaoling landslide triggered by the 1999 Cho-Chi earthquake, Taiwan. Eng. Geol. 68, 259–273.
Chigira, M., 2009. September 2005 rain-induced catastrophic rockslides on slopes affected by deep-seated gravitational deformations, Kyushu, Southern Japan. Eng. Geol. 108, 1–15.
Chigira, M., Wu, X., Inokuchi, T., Wang, G., 2010. Landslides induced by the 2008 Wenchuan earthquake, Sichuan, China. Geomorphology 118, 225–238.
Chigira, M., Tsou, Ch.Y., Matsushi, Y., Hiraishi, N., Matsuzawa, M., 2013. Topographic precursors and geological structures of deep-seated catastrophic landslides caused by Typhoon Talas. Geomorphology 201, 479–493.
Delacourt, C., Allemand, P., Berthier, B., Raucoules, R., Casson, B., Grandjean, P., Pambrun, P., Varel, E., 2007. Remote-sensing techniques for analyzing landslide kinematics: a review. Bulletin de la Société Géologique de France 178, 89–100.
Dikau, R., Brunsden, D., Schrott, D., Ibsen, M.L., 1996. Landslide Recognition: Identification, Movement and Cause. Wiley, Chichester.
Di Luzio, E., Saroli, M., Esposito, C., Bianchi-Fasani, G., Cavinato, G.P., Scarascia-Mugnozza, G., 2004. Influence of structural framework on mountain slope deformation in the Maiella anticline (Central Apennines, Italy). Geomorphology 60, 417–432.
Dramis, F., Sorriso-Valvo, M., 1994. Deep-seated gravitational slope deformations, related landslides and tectonics. Eng. Geol. 38, 231–243.
Dunai, T.J., 2010. Cosmogenic Nuclides, Principles, Concepts and Applications in the Earth Surface. Cambridge University Press, Sciences.
Dunning, S.A., Rosser, N.J., McColl, S.T., Reznichenko, N.V., 2015. Rapid sequestration of rock avalanche deposits within glaciers. Nat. Commun. 6, 7964.
Eberhardt, E., Bonzanigo, L., Loew, S., 2007. Long-term investigation of a deep-seated creeping landslide in crystaline rocks. Part II. Mittigation measures and numerical modelling of deep drainage at Campo Vallemaggia. Can. Geotech. J. 44, 1181–1199.
El Bedoui, S., Guglielmi, Y., Lebourg, T., Pérez, J.-L., 2009. Deep-seated failure propagation in a fractured rock slope over 10,000 years: the La Clapière slope, the south-eastern French Alps. Geomorphology 105, 232–238.
Esposito, C., Bianchi Fasani, G., Martino, S., Scarcascia-Mugnozza, G., 2013. Quaternary gravitational morpho-genesis of Central Apennines (Italy): insights from the Mt. Genzana case history. Tectonophysics 605, 96–103.
Evans, S.G., Clague, J.J., 1993. Glacier-related hazards and climate change. In: Bras, R. (Ed.), The World at Risk: Natural Hazards and Climate Change. American Institute of Physics Conference Proceedings. Vol. 277, pp. 48–60.
Fantucci, R., Sorriso-Valvo, M., 1999. Dendrogeomorphological analysis of a slope near Lago, Calabria (Italy). Geomorphology 30, 165–174.
Federico, A., Popescu, M., Elia, G., Fidelibus, C., Internò, G., Murianni, A., 2012. Prediction of time to slope failure: a general framework. Environ. Earth Sci. 66, 245–256.
Geertsema, M., Hungr, O., Schwab, J.W., Evans, S.G., 2006. A large rockslide-debris avalanche in cohesive soil at Pink Mountain, Northeastern British Columbia, Canada. Eng. Geol. 83, 64–75.
Glade, T., Crozier, M.J., 2005. The nature of landslide hazard impact. In: Glade, T., Anderson, M.G., Crozier, M.J. (Eds.), Landslide Hazard and Risk. John Wiley &Sons Ltd., Chichester, pp. 43–74.
Gori, S., Falcucci, E., Dramis, F., Galadini, F., Galli, P., Giaccio, B., Messina, P., Pizzi, A., Sposato, A., Cosentino, D., 2014. Deep-seated gravitational slope deformation, large-scale rock failure, and active normal faulting along Mt. Morrone (Sulmona basin, Central Italy): geomorphological and paleoseismological analyses. Geomorphology 208, 88–101.
Gosse, J.C., Phillips, F.M., 2001. Terrestrial in situ cosmogenic nuclides: theory and application. Quat. Sci. Rev. 20, 1475–1560.
Guallini, L., Brozzetti, F., Marinangeli, L., 2012. Large-scale deformational systems in the South Polar layered deposits (Promethei Lingula, Mars): "soft-sediment" and deep-seated gravitational slope deformations mechanisms. Icarus 220, 821–843.
Guglielmi, Y., Cappa, F., 2010. Regional-scale relief evolution and large landslides: insights from geomechanical analyses in the Tinée Valley (southern French Alps). Geomorphology 117, 121–129.
Gutiérrez-Santolalla, F., Acosta, E., Ríos, S., Guerrero, J., Lucha, P., 2005. Geomorphology and geochronology of sackung features (uphill-facing scarps) in the Central Spanish Pyrenees. Geomorphology 69, 298–314.
Gutiérrez, F., Ortuño, M., Lucha, P., Guerrero, J., Acosta, E., Coratza, P., Piacentini, D., Soldati, M., 2008. Late Quaternary episodic displacement on a sackung scarp in the central Spanish Pyrenees. Secondary paleoseismic evidence? Geodin. Acta 21, 187–202.
Gutiérrez, F., Carbonel, D., Guerrero, J., McCalpin, J.P., Linares, R., Roqué, C., Zarroca, M., 2012a. Late Holocene episodic displacement on fault scarps related to interstratal dissolution of evaporites (Teruel Neogene Graben, NE Spain). J. Struct. Geol. 34, 2–19.
Gutiérrez, F., Linares, R., Roqué, C., Zarroca, M., Rosell, J., Galve, J.P., Carbonell, D., 2012b. Investigating gravitational grabens related to lateral spreading and evaporite dissolution subsidence by means of detailed mapping, trenching, and electrical resistivity tomography (Spanish Pyrenees). Lithos 4, 331–353.
Hasler, A., Gruber, S., Beutel, J., 2012. Kinematics of steep bedrock permafrost. J. Geophys. Res. 117, F01016.
Hauswirth, E., Pirkl, H., Roch, K., Scheidegger, A.E., 1979. Untersuchungen eines Talzuschubes bei Lesach (Kals, Osttirol). Verh. Geol. Bundesanst. 2, 51–76.
Herman, F., Seward, D., Valla, P.G., Carter, A., Kohn, B., Willett, S.D., Ehlers, T.A., 2013. Worldwide acceleration of mountain erosion under a cooling climate. Nature 504, 423–426.
Hermanns, R., Oppikofer, T., Dahle, H., Eiken, T., Ivy-Ochs, S., Blikra, L., 2013. Understanding long-term slope deformation for stability assessment of rock slopes: the case of the Oppstadhornet rockslide, Norway. Ital. J. Eng. Geol. Environ. Book Ser. 6, 255–264.
Hewitt, K., 2006. Rock avalanches with complex run out and emplacement, Karakoram Himalaya, Inner Asia. In: Evans, S.G., Scarascia Mugnozza, G., Strom, A.L., Hermanns, R.L. (Eds.), Landslides From Massive Rock Slope FailureProc.NATO Advanced Workshop, Celano, Italy, June Vol. 2002. Springer-Verlag, Dordrecht, pp. 521–550.
Hewitt, K., Clague, J., Orwin, J.F., 2008. Legacies of catastrophic rock slope failures in mountain landscapes. Earth Sci. Rev. 87, 1–38.
Hippolyte, J.C., Brocard, G., Tardy, M., Nicoud, G., Bourlès, D., Braucher, R., Ménard, G., Souffaché, B., 2006. The recent fault scarps of the Western Alps (France): tectonic surface ruptures or gravitational sackung scarps? A combined mapping, geomorphic, levelling, and ^{10}Be dating approach. Tectonophysics 418, 255–276.
Hippolyte, J.C., Bourlès, D., Braucher, R., Carcaillet, J., Léanni, L., Arnold, M., Aumaitre, G., 2009. Cosmogenic ^{10}Be dating of a sackung and its faulted rock glaciers, in the Alps of Savoy (France). Geomorphology 108, 312–320.
Hippolyte, J.C., Bourlès, D., Léanni, L., Braucher, R., Chauvet, F., Lebetard, A.E., 2012. ^{10}Be ages reveal >12 ka of gravitational movement in a major sackung of the Western Alps (France). Geomorphology 171–172, 139–153.
Holm, K., Bovis, M., Jakob, M., 2004. The landslide response of alpine basins to post-Little Ice Age glacial thinning and retreat in southwestern British Columbia. Geomorphology 57, 201–216.

Hughes, P.D., Gibbard, P.L., Ehlers, J., 2013. Timing of glaciation during the last glacial cycle: evaluating the concept of a global 'Last Glacial Maximum' (LGM). Earth Sci. Rev. 125, 171–198.
Hungr, O., Leroueil, S., Picarelli, L., 2014. The Varnes classification of landslide types, an update. Landslides 11, 167–194.
Jaboyedoff, M., Couture, R., Locat, P., 2009. Structural analysis of Turtle Mountain (Alberta) using digital elevation model: toward a progressive failure. Geomorphology 103, 5–16.
Jarman, D., 2006. Large rock slope failures in the highlands of Scotland: characterisation, causes and spatial distribution. Eng. Geol. 83, 161–182.
Jarman, D., Calvet, M., Corominas, J., Delmas, M., Gunnell, Y., 2014. Large-scale rock slope failures in the eastern Pyrenees: identifying a sparse but significant population in paraglacial and parafluvial contexts. Geograf. Ann. Ser. A Phys. Geogr. 96, 357–391.
Jibson, R.W., Harp, E.L., Schulz, W., Keefer, D.K., 2004. Landslides triggered by the 2002 Denali fault, Alaska earthquake and the inferred nature of the strong shaking. Earthquake Spectra 20, 669–691.
Jomard, H., Lebourg, T., Guglielmi, Y., 2014. Morphological analysis of deep-seated gravitational slope deformation (DSGSD) in the western part of the argentera massif. A morpho-tectonic control? Landslides 11, 107–117.
Kellerer-Pirklbauer, A., Proske, H., Strasser, V., 2010. Paraglacial slope adjustment since the end of the last glacial maximum and its long-lasting effects on secondary mass wasting processes: Hauser Kaibling, Austria. Geomorphology 120, 65–76.
Kemeny, J., 2003. The time-dependent reduction of sliding cohesion due to rock bridges along discontinuities: a fracture mechanics approach. Rock Mech. Rock. Eng. 36, 27–38.
Klimeš, J., Rowberry, M.D., Blahůt, J., Briestenský, M., Hartvich, F., Košťák, B., Rybář, J., Stemberk, J., Štěpančíkova, P., 2012. The monitoring of slow-moving landslides and assessment of stabilization measures using an optical-mechanical crack gauge. Landslides 9, 407–415.
Korup, O., 2005. Large landslides and their effect on sediment flux in South Westland, New Zealand. Earth Surf. Process. Landf. 30, 305–323.
Korup, O., 2006. Effects of large deep-seated landslides on hillslope morphology, Western Southern Alps, New Zealand. J. Geophys. Res. 111, F01018.
Korup, O., Clague, J.J., Hermanns, R.L., Hewitt, K., Strom, A.L., Weidinger, J.T., 2007. Giant landslides, topography, and erosion. Earth Planet. Sci. Lett. 261, 578–589.
Košťák, B., Avramova-Tacheva, E., 1981. Propagation of coastal slope deformations at Taukliman, Bulgaria. Int. Assoc. Eng. Geol. Bull. 23, 67–73.
Kromuszczyńska, O., Makowska, M., Dębniak, K., 2014. Valles Marineris — a place full of answers. In: Zielinski, T., et al. (Eds.), Insights on Environmental Changes, Where the World is Heading. Springer, pp. 17–32.
Lacroix, P., Amitrano, D., 2013. Long-term dynamics of rockslides and damage propagation inferred from mechanical modeling. J. Geophys. Res. Earth Surf. 118, 2292–2307.
Lambiel, C., Delaloye, R., 2004. Contribution of real-time kinematic GPS in the study of creeping mountain permafrost: examples from the Western Swiss Alps. Permafr. Periglac. Process. 15, 229–241.
Lebourg, T., M., Hernandez, H., Jomard, S., El Bedoui, T., Bois, S., Zerathe, E., Tric, M., Vidal, 2011. Temporal evolution of weathered cataclastic material in gravitational faults of the La Clapiere deep-seated landslide by mechanical approach. Landslides 8, 241–252.
Lebourg, T., Zerathe, S., Fabre, R., Giuliano, J., Vidal, M., 2014. A Late Holocene deep-seated landslide in the northern French Pyrenees. Geomorphology 208, 1–10.
Lenti, S., Martino, A., Paciello, A., Prestininzi, A., Rivellino, S., 2012. Microseismicity within a karstified rock mass due to cracks and collapses as a tool for risk management. Nat. Hazards 64, 359–379.
Le Roux, O., Schwartz, S., Gamond, J.F., Jongmans, D., Bourles, D., Braucher, R., Mahaney, W., Carcaillet, J., Leanni, L., 2009. CRE dating on the head scarp of a major landslide (Séchilienne, French Alps), age constraints on Holocene kinematics. Earth Planet. Sci. Lett. 280, 239–245.
Le Roux, O., Jongmans, D., Kasperski, J., Schwartz, S., Potherat, P., Lebrouc, V., Lagabrielle, R., Meric, O., 2011. Deep geophysical investigation of the large Séchilienne landslide (Western Alps, France) and calibration with geological data. Eng. Geol. 120, 18–31.
Lu, Z.-Y., Rollerson, T., Geertsema, M., 2003. The Mosque Mountain rock slide, Sustut watershed, Fort St. James, Northern British Columbia, Canada. 3rd Canadian Conference on Geotechnique and Natural Hazards, Edmonton, AB, p. 325.
MacFarlane, D.F., 2009. Observations and predictions of the behavior of large, slow moving landslides in schist, Clyde Dam reservoir, New Zealand. Eng. Geol. 109, 5–15.
Makos, M., Dzierżek, J., Nitychoruk, J., Zreda, M., 2014. Timing of glacier advances and climate in the High Tatra Mountains (Western Carpathians) during the last glacial maximum. Quat. Res. 82, 1–13.
Malgot, J., 1977. Deap-seated gravitational slope deformations in neovolcanic mountain ranges of Slovakia. Bull. Eng. Geol. Environ. 16, 106–109.
Mantovani, M., Devoto, S., Forte, E., Mocnik, A., Pasuto, A., Piacentini, D., Soldati, M., 2013. A multidisciplinary approach for rock spreading and block sliding investigation in the north-western coast of Malta. Landslides 10, 611–622.
Margielewski, W., 2006. Records of the Late Glacial–Holocene palaeoenvironmental changes in landslide forms and deposits of the Beskid Makowski and Beskid Wyspowy Mts. area (Polish Outer Carpathians). Folia Quat. 76, 1–149.
Marschallinger, R., Eichkitz, C., Gruber, H., Heibl, K., 2009. The Gschliefgraben landslide (Austria): a remediation approach involving torrent and avalanche control, geology, geophysics, geotechnics and geoinformatics. Aust. J. Earth Sci. 102, 36–51.
Massey, Ch., McSaveney, M., Davies, T., 2013. Evolution of an overflow channel across the Young River landslide dam, New Zealand. In: Margottini, C., et al. (Eds.), Landslide Science and Practice Vol 6. Springer, New York, pp. 43–49.
McCalpin, J.P., 2009. Paleoseismology. second ed. Academic Press, San Diego.
McCalpin, J.P., Irvine, J.R., 1995. Sackungen at the Aspen highlands ski area, Pitkin County, Colorado. Environ. Eng. Geosci. 1, 277–290.
McCalpin, J.P., Hart, E.W., 2003. Ridge-top spreading features and relationship to earthquakes, San Gabriel Mountains region, Southern California—parts A and B. In: Hart, E.W. (Ed.), Ridge-Top Spreading in California; Contributions Toward Understanding a Significant Seismic Hazard: Sacramento, California, California Geological Survey, CD 2003–05, 2 CD-ROMs.
McCalpin, J.P., Bruhn, R.L., Pavlis, T.L., Gutierrez, F., Guerrero, J., Lucha, P., 2011. Antislope scarps, gravitational spreading, and tectonic faulting in the western Yakutat microplate, south coastal Alaska. Geosphere 7, 1143–1158.
McColl, S.T., 2012. Paraglacial rock-slope stability. Geomorphology 153–154, 1–16.
McColl, S.T., Davies, T.R.H., 2013. Large ice-contact slope movements: glacial buttressing, deformation and erosion. Earth Surf. Process. Landf. 38, 1102–1115.
McDougall, S., Boultbee, N., Hungr, O., Stead, D., Schwab, J.W., 2006. The Zymoetz River landslide, British Columbia, Canada: description and dynamics of a rock slide-debris flow. Landslides 3, 195–204.
Mège, D., Bourgeois, O., 2011. Equatorial glaciations on Mars revealed by gravitational collapse of Valles Marineris wallslopes. Earth Planet. Sci. Lett. 310, 182–191.
Mège, D., Le Deit, L., Rango, T., Korme, T., 2013. Gravity tectonics of topographic ridges: halokinesis and gravitational spreading in the Western Ogaden, Ethiopia. Geomorphology 193, 1–13.
Moro, M., Saroli, M., Salvi, S., Stramondo, S., Doumaz, F., 2007. The relationship between seismic deformation and deep-seated gravitational movements during the 1997 Umbria-Marche (Central Italy) earthquakes. Geomorphology 89, 297–307.
Moro, M., Saroli, M., Tolomei, C., Salvi, S., 2009. Insights on the kinematics of deep-seated gravitational slope deformations along the 1915 Avezzano earthquake fault (Central Italy), from time-series DInSAR. Geomorphology 112, 261–276.
Moro, M., Saroli, M., Gori, S., Falcucci, E., Galadini, F., Messina, P., 2012. The interaction between active normal faulting and large scale gravitational mass movements revealed by paleoseismological techniques: a case study from central Italy. Geomorphology 151–152, 164–174.
Moser, M., Meier, H., Lotter, M., Weidner, S., 2002. Geotechnical aspects of deep-seated mass movements in Austria. In: Rybář, J., Stemberk, J., Wagner, P. (Eds.), Landslides. Swets and Teitlinger, Lisse, pp. 423–429 (ISBN: 905809393).
Němčok, A., 1972. Gravitational slope deformation in high mountains. Proceedings of the 24th International Geological Congress. Montreal. Vol. 13, pp. 132–141.
Němčok, A., 1982. Zosuvy v slovenských Karpatoch (landslides in the Slovakian Carpathians). Publ. VEDA, Bratislava. (in Slovak, with English Summary).
Newman, S.D., 2013. Deep-Seated Gravitational Slope Deformations Near the Trans-Alaska Pipeline, East-Central Alaska Range Master thesis Simon Fraser University, Burnaby, p. 243.
Nishii, R., Matsuoka, N., Daimaru, H., Yasuda, M., 2013. Precursors and triggers of an alpine rockslide in Japan: the 2004 partial collapse during a snow-melting period. Landslides 10, 75–82.
Novosad, S., 1956. Fosilní rozeklání hřbetu Lukšinec u Lysé hory (in Czech). Časopis pro mineralogii a geologii. 1, 126–131.
Novosad, S., 1966. Porušení svahů v godulských vrstvách Moravskoslezských Beskyd (in Czech). Sborník Geologických Věd, Hydrogeologie–Inženýrská Geologie 5, 71–86.
Novosad, S., 2002. Key-role of monitoring landslide for risk management. — Paper Presented at the 1st European Conference on Landslides, June 24–26, 2002, 1–20, Prague, 2002.
Pánek, T., Hradecký, J., Minár, J., Hungr, O., Dušek, R., 2009a. Late Holocene catastrophic slope collapse affected by deep-seated gravitational deformation in flysch: Ropice Mountain, Czech Republic. Geomorphology 103, 414–429.
Pánek, T., Hradecký, J., Šilhán, K., Smolková, V., Altová, V., 2009b. Time constraints for the evolution of a large slope collapse in karstified mountainous terrain (case study from the southwestern tip of the Crimean Mountains, Ukraine). Geomorphology 108, 171–181.
Pánek, T., Tábořík, P., Klimeš, J., Komárková, V., Hradecký, J., Šťastný, M., 2011a. Deep-seated gravitational slope deformations in the highest parts of the Czech Flysch Carpathians: evolutionary model based on kinematic analysis, electrical imaging and trenching. Geomorphology 129, 92–112.
Pánek, T., Šilhán, K., Tábořík, P., Hradecký, J., Smolková, V., Lenart, J., Brázdil, R., Kašičková, L., Pazdur, A., 2011b. Catastrophic slope failure and its origins: case of the May 2010 Girová Mountain long-runout rockslide (Czech Republic). Geomorphology 130, 352–364.
Pánek, T., Smolková, V., Hradecký, J., Baroň, I., Šilhán, K., 2013. Holocene reactivations of catastrophic complex flow-like landslides in the Flysch Carpathians (Czech Republic/Slovakia). Quat. Res. 80, 33–46.
Pánek, T., 2015. Recent progress in landslide dating: a global overview. Prog. Phys. Geogr. 39, 168–198.
Pedrazzini, A., Jaboyedoff, M., Loye, A., Derron, M.H., 2013. From deep seated slope deformation to rock avalanche: destabilization and transportation models of the Sierre landslide (Switzerland). Tectonophysics 605, 149–168.
Preisig, G., Eberhardt, E., Smithyman, M., Preh, A., Bonzanigo, L., 2016. Hydromechanical rock mass fatigue in deep-seated landslides accompanying seasonal variations in pore pressures. Rock Mech. Rock. Eng. http://dx.doi.org/10.1007/s00603-016-0912-5.
Pinto, L., Hérail, G., Sepúlveda, S.A., Krop, P., 2008. A Neogene giant landslide in Tarapaca, northern Chile: A signal of instability of the westernmost Altiplano and palaeoseismicity effects. Geomorphology 102, 532–541.
Radbruch-Hall, D., 1978. Gravitational creep of rock masses on slopes. In: Voight, B. (Ed.), Rockslides and Avalanches — Natural PhenomenaDevelopments in Geotechnical Engineering Vol. 14. Elsevier, Amsterdam, pp. 608–657.
Reitner, J., Linner, M., 2009. Formation and preservation of large scale toppling related to alpine tectonic structures — Eastern Alps. Aust. J. Earth Sci. 102, 69–80.
Remondino, F., Barazzetti, L., Nex, F., Scaioni, M., Sarazzi, D., 2011. UAV Photogrammetry for Mapping and 3D Modeling — Current Status and Future Perspectives. International

Archives of the Photogrammetry, Remote Sensing and Spatial Information Sciences, Volume XXXVIII-1/C22, 2011 ISPRS Zurich 2011 Workshop, 14–16 September 2011, Zurich, Switzerland. p. 7.
Rizzo, V., Leggeri, M., 2004. Slope instability and sagging reactivation at Maratea (Potenza, Basilicata, Italy). Eng. Geol. 71, 181–198.
Rohn, J., Resch, M., Schneider, H., Fernadez–Steeger, T.M., Czurda, K., 2004. Large-scale lateral spreading and related mass movements in the Northern Calcareous Alps. Bull. Eng. Geol. Environ. 63, 71–75.
SafeLand deliverable 4.1, (2010) Review of Techniques for Landslide Detection, fast Characterization, Rapid Mapping and Long-term Monitoring, in: Michoud, C., Abellán, A., Derron, M.-H., Jaboyedoff, M. (eds), (http://www.safeland-fp7.eu (last visited 30.10.2014))
Sakals, M.E., Geertsema, M., Schwab, J.W., Foord, V.N., 2012. The Todagin Creek landslide of October 3, 2006, Northwest British Columbia, Canada. Landslides 9, 107–115.
Sanchez, G., Rolland, Y., Corsini, M., Braucher, R., Bourlès, D., Arnold, M., Aumaître, G., 2010. Relationships between tectonics, slope instability and climate change: cosmic ray exposure dating of active faults, landslides and glacial surfaces in the SW Alps. Geomorphology 117, 1–13.
Seijmonsbergen, A.C., Woning, M.P., Verhoef, P.N.W., de Graaf, L.W.S., 2005. The failure mechanism of a Late Glacial Sturzstrom in the Subalpine Molasse (Leckner Valley, Voralberg, Austria). Geomorphology 66, 277–286.
Shroder, J.F., Owen, L.A., Seong, Y.B., Bishop, M.P., Bush, A., Caffee, M.C., Copland, L., Finkel, R.C., Kamp, U., 2011. The role of mass movements on landscape evolution in the Central Karakoram: discussion and speculation. Quat. Int. 236, 34–47.
Sorriso-Valvo, M., Antronico, L., Gullà, G., Tansi, C., Amelio, M., 1999. Mass movement,geologic structure and morphologic evolution of the Pizzotto-Greci slope (Calabria,Italy). Geomorphology 31, 147–163.
Strozzi, T., Ambrosi, Ch., Raetzo, H., 2013. Interpretation of aerial photographs and satellite SAR interferometry for the inventory of landslides. Remote Sens. 5, 2554–2570.
Tamburini, A., Del Conte, S., Larini, G., Lopardo, L., Malaguti, C., Vescovi, P., 2011. Application of SqueeSARTM to the characterization of deep seated gravitational slope deformations: the Berceto case study (Parma, Italy). In: Margottini, C., Canuti, P., K., Sassa (Eds.), Landslide Science and Practice, Vol. 2 — Early Warning, Instrumentation and Monitoring. Springer, New York, pp. 437–444.
Thompson, S.C., Clague, J.J., Evans, S.G., 1997. Holocene activity of the Mt. Currie scarp, Coast Mountains, British Columbia, and implications for its origin. Environ. Eng. Geosci. 3, 329–348.
Tibaldi, A., Pasquarè, F.A., 2008. Quaternary deformations along the 'Engadine–Gruf tectonic system', Swiss–Italian Alps. J. Quat. Sci. 23, 475–487.
Tibaldi, A., Rovida, A., Corazzato, C., 2004. A giant deep-seated slope deformation in the Italian Alps studied by paleoseismological and morphometric techniques. Geomorphology 58, 27–47.
Tolomei, C., Taramelli, A., Moro, M., Saroli, M., Aringoli, D., Salvi, S., 2013. Analysis of the deep-seated gravitational slope deformations over Mt. Frascare (Central Italy) with geomorphological assessment and DInSAR approaches. Geomorphology 201, 281–292.
Turnbull, J.M., Davies, T.R.H., 2006. A mass movement origin for cirques. Earth Surf. Process. Landf. 31, 1129–1148.
Turner, D., Lucieer, A., de Jong, S.M., 2015. Time series analysis of landslide dynamics using an unmanned aerial vehicle (UAV). Remote Sens. 7, 1736–1757.
Unkel, I., Ehret, D., Rohn, J., 2013. Recurrence analysis of the mass movement activity at stambach (Austria) based on ^{14}C dating. Geomorphology 190, 103–111.
Urban, J., Margielewski, W., Hercman, H., Žák, K., Zernitskaya, V., Pawlak, J., 2013. Dating speleothems in sandstone, non-karst caves — methodological aspects and practical application, Polish Outer Carpathians case study. In: Migoń, P., Kasprzak, M. (Eds.), Sandstone Landscapes, Diversity, Ecology and Conservation, Proceedings of the 3rd International Conference on Sandsone Landscapes, Kudowa-Zdrój, Poland, 25–28 April 2012, pp. 192–201.
Vallet, A., Charlier, J.B., Fabbri, O., Bertrand, C., Carry, N., Mudry, J., 2016. Functioning and precipitation–displacement modelling of rainfall-induced deep-seated landslides subject to creep deformation. Landslides http://dx.doi.org/10.1007/s10346-015-0592-3 (in press).
Varnes, D.J., Radbruch-Hall, D.H., Varnes, K.L., Smith, W.K., Savage, W.Z., 1990. Measurement of ridge-spreading movements (Sackungen) at Bald Eagle Mountain, Lake County, Colorado, 1975–1989. U.S. Geological Survey Open File Report 90-543: U.S. Geological Survey, Denver, CO (13 p).
Vilímek, V., Zvelebil, J., Klimeš, J., Patzelt, Z., Astete, F., Kachlík, V., Hartvich, F., 2007. Geomorphological research of large-scale slope instability at Machu Picchu, Peru. Geomorphology 89, 241–257.
Walker, M., 2005. Quaternary Dating Methods. John Wiley & Sons, Chichester.
Wang, N.W., Chigira, M., Furuya, T., 2003. Geological and geomorphological precursors of the Chiu-fen-erh-shan landslide triggered by the Chi-chi earthquake in central Taiwan. Eng. Geol. 69, 1–13.
Wilson, A.J., Petley, D.N., Murphy, W., 2003. Down-slope variation in geotechnical parameters and pore fluid control on a large-scale Alpine landslide. Geomorphology 54, 49–62.
Woschitz, H., Brunner, F., 2008. Monitoring a deep-seated mass movement using large strain rosette. 4th IAG Symposium on Geodesy for Geotechnical and Structural Engineering LNEC, Lisbon 2008, May 12–15, p. 10.
Yin, Y., Zhu, J., Yang, S., 2011. Research on catastrophic rock avalanche at Guanling, Guizhou, China. Landslides 8, 517–525.
Záruba, Q., Mencl, V., 1969. Landslides and Their Control. Academia, Prague.
Zerathe, S., Lebourg, T., 2012. Evolution stages of large deep-seated landslides at the front of a subalpine meridional chain (Maritime-Alps, France). Geomorphology 138, 390–403.
Zerathe, S., Braucher, R., Lebourg, T., Bourlès, D., Manetti, M., Leanni, L., 2013. Dating chert (diagenetic silica) using in-situ produced ^{10}Be: possible complications revealed through the comparison with ^{36}Cl applied on coexisting limestone. Quat. Geochronol. 17, 81–93.
Zerathe, S., Lebourg, T., Braucher, R., Bourlés, D., 2014. Mid-Holocene cluster of large-scale landslides revealed in the Southwestern Alps by ^{36}Cl dating. Insight on an Alpine-scale landslide activity. Quat. Sci. Rev. 90, 106–127.
Zhou, J.W., Cui, P., Hao, M.H., 2015. Comprehensive analyses of the initiation and entrainmnt processes of the 2000 Yigong catastrophic landslide in Tibet, China. Landslides http://dx.doi.org/10.1007/s10346-014-0553-2.
Zischinsky, U., 1966. On the deformation of high slopes. Proc. Lst Conf. Int. Soc. Rock Mech., Lisbon, Sect., 2, pp. 179–185.
Zischinsky, U., 1969. Über sackungen. Rock Mech. 1, 30–52.